Machine Learning Identifies Microbiome and Clinical Predictors of Sustained Weight Loss Following Prolonged Fasting

Gelsomina N. Kaufhold[1,2,3,4]*, Theda U. P. Bartolomaeus[1,2,3,4,5,*], Kristin Kräker[1,2,3,4], Till Schütte[1,2,3,4], Sakshi Kamboj[6], Ulrike Löber[1,2,3,4], Gabriele Rahn[1], Victoria McParland[1,3,7], Lena Braun[1], Lajos Markó[1,2,3,4], Matanat Mammadli[1,2,3], Alexander Krannich[8], Lina S. Bahr[1,2,3], Friederike Gutmann[1,2,3,4], Friedemann Paul[1,2,3], Quinten R. Ducarmon[9,10], Georg Zeller[9,10], Robin Mesnage[11,12], Nicola Wilck[1,3,4,7], Alma Zernecke[13], Peter J. Oefner[6], Wolfram Gronwald[6], Dominik N. Müller[1,2,3,4], Sofia K. Forslund-Startceva[1,2,3,4,9], Sylvia Bähring[1,2,3,†], Hendrik Bartolomaeus[3,4,13,†], Nadja Siebert[1,2,3,†]

[1]Experimental and Clinical Research Center (ECRC), a cooperation of Charité - Universitätsmedizin Berlin and Max Delbrück Center for Molecular Medicine, Berlin, Germany

[2]Charité-Universitätsmedizin Berlin, corporate member of Freie Universität Berlin and Humboldt-Universität zu Berlin, Berlin, Germany.

[3]Max Delbrück Center for Molecular Medicine in the Helmholtz Association (MDC), Berlin, Germany

[4]DZHK (German Centre for Cardiovascular Research), partner site Berlin, Germany

[5]Centre for Ecological and Evolutionary Synthesis (CEES), Department of Biosciences, University of Oslo, Oslo, Norway.

[6]Institute of Functional Genomics, University of Regensburg, Regensburg, Germany

[7]Department of Nephrology and Internal Intensive Care Medicine, Charité –Universitätsmedizin Berlin, Germany.

[8]BioStats GmbH, Nauen, Germany

[9]Molecular Systems Biology Unit, European Molecular Biology Laboratory (EMBL), Heidelberg, Germany.

[10]Leiden University Center for Infectious Diseases (LUCID), Leiden University Medical Center (LUMC), Leiden, Netherlands

[11]Science Department, Buchinger Wilhelmi Clinic, Überlingen, Germany.

[12]Department of Nutritional Sciences, School of Life Course Sciences, Faculty of Life Sciences and Medicine, King's College London, London, United Kingdom.

[13]Institute of Experimental Biomedicine, University Hospital Würzburg, Germany.

*contributed equally

†jointly supervised the work

Correspondence: bartolomae_h@ukw.de

Abstract

Background: Prolonged fasting may improve metabolic health, but controlled data in healthy adults with longer follow-up and multi-omics profiling are limited. We investigated short- and long-term effects of a 5-day fasting intervention on body composition, gut microbiome, and circulating and fecal metabolites, and assessed whether baseline characteristics predict individual weight-loss response.

Methods: In a randomized, waitlist-controlled trial, 38 healthy adults completed a 5-day fasting intervention with 12-week follow-up (LEANER study). Outcomes included body mass index and body composition, gut microbiome composition, and plasma and fecal metabolites. Changes over time and between groups were evaluated using regression-based models and paired non-parametric tests, as appropriate. Additionally, permutation-based multivariate testing was performed on microbiome and metabolome data. Twelve-week body weight response was predicted using data-driven machine learning with cross-validation, followed by external validation in three independent cohorts undergoing prolonged fasting protocols.

Results: Fasting reduced body mass index acutely, predominantly driven by loss of fat mass, and these improvements partially persisted at 12 weeks. Fasting induced marked shifts in gut microbiome composition and in plasma and fecal metabolites. Post-fasting and longer-term changes in microbial diversity were associated with baseline microbiome diversity. A model combining baseline microbiome and clinical variables predicted body mass index response at 12 weeks; prominent predictors included an unclassified *Faecalibacterium* species, *Oscillibacter* sp. 50_27, low-density lipoprotein cholesterol, and systolic blood pressure. The model generalized to three independent cohorts, including individuals with metabolic

syndrome, patients with multiple sclerosis exposed to repeated fasting, and healthy volunteers fasting for 6–12 days.

Conclusions: In healthy adults, a 5-day prolonged fasting intervention produces robust short-term metabolic changes with partial persistence and consistent remodeling of the gut microbiome and metabolite profiles. Baseline microbiome and clinical characteristics can help stratify expected longer-term responses, supporting the development of individualized fasting-based interventions.

Trial registration: ClinicalTrials.gov, NCT04452916. Registered on June 29, 2020

Key words: fasting, gut microbiome, weight loss, machine learning, personalized nutrition, precision medicine, multi-omics, prevention, metabolic health

68 **Introduction**

69 Fasting interventions have gained renewed attention for their potential to modulate
70 metabolism, reshape the gut microbiome, and promote healthy aging[1]. While fasting
71 protocols vary widely from time-restricted eating to fasting-mimicking diets[2], and prolonged
72 food abstinence lasting up to several weeks (up to 26 days)[3], the underlying principle is
73 consistent: transient caloric deprivation triggers coordinated physiological responses that
74 may confer long-term health benefits[4].

75 Evidence from patient populations, including those with metabolic syndrome[5], autoimmune
76 diseases[6,7], and cancer[8], suggests that fasting can influence key regulatory pathways such as
77 autophagy, insulin sensitivity, and oxidative stress[1]. In individuals with metabolic syndrome,
78 we previously demonstrated that a 5-day fast atop a DASH (Dietary Approaches to Stop
79 Hypertension) diet induced profound and coordinated changes in gut microbiome
80 composition and immune cell states most of which were reversed at 12 weeks follow-up[5].
81 Using immune cell population or microbiome profiles, we developed models that predicted
82 long-term antihypertensive effects, supporting the concept of data-driven stratification[5].

83 Metabolic effects of weight loss interventions such as fasting may be assessed by
84 determination of resting energy expenditure (REE). REE is defined as the energy required to
85 sustain vital physiological functions while at rest and without any external activity or food
86 intake[9]. It accounts for approximately 60–75% of total daily energy expenditure and is the
87 most significant contributor to overall metabolism[9]. The value is influenced by factors
88 including age, sex, genetics, and body composition, with lean muscle mass being a dominant
89 determinant[10]. Changes in REE are central to understanding metabolic adaptations and the
90 effects of interventions, whether nutritional, pharmacological, or involving lifestyle changes.
91 Reliable measurement is typically achieved through indirect calorimetry, considered the gold

92 standard[11,12]. Changes in REE may reflect body responses to interventions and contribute to
93 understanding individual variability in weight management and energy requirements.
94 In parallel, gut microbiome profiling has emerged as a powerful tool for personalized
95 medicine[13]. Microbial signatures have been linked to energy metabolism[14], weight
96 regulation[15,16], and immune modulation[17,18]. Personalized dietary approaches that account
97 for microbiome composition have demonstrated superior outcomes in metabolic control[8].
98 Emerging applications extend to autoimmune, neuropsychiatric, and oncologic indications,
99 underscoring the potential of microbiome-informed strategies in precision medicine[13,19].
100 Despite these advances, the long-term effects of prolonged fasting in healthy individuals
101 remain poorly characterized. Most existing studies rely on non-randomized designs, lack
102 adequate control groups, or fail to include follow-up assessments. Furthermore, many
103 interventions are performed in multimodal clinical settings involving exercise, psychological
104 support, and dietary coaching[5], making it difficult to isolate the effect of fasting alone.
105 Here, we present a randomized, waitlist-controlled study investigating the effects of a 5-day
106 prolonged fasting intervention in healthy adults, with follow-up assessments at 12 weeks. We
107 integrated clinical, microbiome, and metabolome profiling to characterize immediate and
108 long-term physiological responses. Using machine learning (ML), we show that sustained
109 weight loss can be predicted from baseline microbiome and clinical features. Results were
110 validated in one independent healthy cohort and cohorts with metabolic syndrome and
111 multiple sclerosis. Our findings offer mechanistic insight into fasting responses and support
112 the potential of microbiome-informed strategies for personalized lifestyle interventions.
113

Results

Prolonged fasting affects energy expenditure and long-term weight loss

Thirty-eight healthy participants were recruited for a 5-day prolonged fasting intervention (Figure 1a). As fasting interventions cannot be blinded, we decided to use a waiting list control to account for physiological fluctuations within a 12-week timeframe while maximizing the number of participants undergoing prolonged fasting (Figure 1A). Baseline characteristics are shown in Table 1.

Of the 38 participants, 83% reported fasting-related adverse events (AE) (Table S1). All AE were mild and transient and did not necessitate discontinuation of fasting. Blood glucose and β-hydroxybutyrate (BHB) levels were measured each morning and evening during the five-day fasting period (days 1–5), confirming that all participants adhered closely to the study protocol (Figure S1a, b). We observed a diurnal rhythm with higher BHB but lower glucose concentrations in the morning compared to the evening (Figure S1a, b). Continuous interstitial glucose monitoring during the five-day fasting period, compared with baseline measurements and waiting-list controls, confirmed a dynamic reduction in glucose levels over the course of the fasting period (Figure 1b). Following refeeding, the glucose levels normalized; however, between days 2 and 4 post-fast, blood glucose concentrations were elevated throughout the day (06:00–22:00) compared with baseline measurements (Figure 1c).

Our predefined endpoint was a change in REE. Prolonged fasting acutely reduced REE by 62 kcal/d, suggesting a fasting-induced, energy-preserving mechanism (Figure 1d, Supplementary Data 1). We did not observe alterations in REE between the two baseline timepoints of waiting list controls (Figure 1d). Following the findings of earlier work[10], we performed a linear mixed model showing that lean mass ($p < 0.001$) and not self-reported

138 sex significantly influenced REE at all visits, including post-fasting (Figure S2). Following the
139 five-day fast, respiratory exchange ratios (RER) declined significantly (Figure 1e), paralleling a
140 peak in BHB concentrations on day 5 (Figure S1b). All those metabolic markers returned to
141 baseline by 12 weeks post-fast.
142 Furthermore, we observed that prolonged fasting reduced BMI (Figure 1f). This decrease was
143 partly reversed at the 12-week follow-up (Figure 1f). Body composition analysis attributed
144 this incomplete return towards baseline BMI predominantly to a reduction in fat mass
145 (Figure 1g, S1g). Of note, the absolute and relative reduction of body fat was accompanied
146 by a reduction in lean mass during fasting that completely reverted at follow-up (Figure S1h).
147 Prolonged fasting reduced waist-to-hip ratio and diastolic blood pressure while increasing
148 heart rate, findings which are consistent with a previously published study[5] in metabolic
149 syndrome (Figure S1d-g). In contrast to metabolic syndrome patients[5], the healthy
150 participants in this study did not exhibit sustained blood-pressure reduction (Figure S1e, f).
151 Taken together, these results demonstrate that prolonged fasting is well tolerated in healthy
152 individuals, yielding sustained reductions in BMI and fat mass, while most metabolic and
153 hemodynamic parameters return to baseline during the 12-week follow-up.
154
155 *Prolonged fasting induces large short-term and small long-term changes in gut microbiome*
156 *composition*
157 To assess the natural fluctuation of the gut microbiome composition, we analyzed changes
158 between the two baseline samples (baseline 0 and baseline 1) from the waiting list control
159 (Figure 1a). Microbial alpha diversity, measured as Shannon index, and microbiome
160 composition quantified by Bray-Curtis dissimilarity did not differ significantly between the
161 two baseline samples (Figure S3a, b). Shannon index remained stable across all study visits

162 (Figure 2a). In contrast, individual trajectories in response to fasting varied markedly (Figure
163 2a). Interestingly, short-term (post-fasting) and long-term (follow-up) changes in alpha-
164 diversity correlated negatively with alpha-diversity at baseline, implicating baseline
165 differences in microbiome composition as relevant predictors of fasting-induced microbiome
166 changes (Figure 2b, c). Bray-Curtis dissimilarity-based multivariate analysis of the taxonomic
167 composition demonstrated a significant shift in microbial community composition in
168 response to fasting that partially reversed during the follow-up period (Figure 2d). Consistent
169 with the observed shift in the multivariate analysis, fasting induced significant changes in
170 several bacterial species that reversed during follow-up. For example, *Roseburia sp.* inserta
171 sedis and *Bifidobacterium adolescentis* decreased after the fasting period but increased at
172 follow-up, whereas *Faecalibacterium sp.* CAG-74 showed the opposite pattern (Figure 2e,
173 S3c, Supplementary Data 2). In contrast, only seven taxa exhibited sustained abundance
174 changes (Figure S3c).
175 Next, we analyzed gut-specific metabolic modules using GOmixer[20]. Again, fasting induced
176 pronounced alterations that largely reverted to baseline during follow-up (Figure 2f). Only for
177 three modules, ketone body synthesis, osmoprotectant transport system, and
178 N-acetylneuraminate and N-acetylmannosamine degradation, fasting induced a long-lasting
179 increase when comparing baseline to follow-up (Figure 2f, Figure S4a, Supplementary Data
180 3).
181 Overall, prolonged fasting induces pronounced compositional shifts in the gut microbiome,
182 which were largely reversed upon refeeding, resulting in minimal long-term deviations from
183 baseline at the 12-week follow-up. Notably, baseline alpha diversity metrics correlate with
184 the magnitude of alpha diversity changes both immediately after fasting and at follow-up.
185

186 *Prolonged fasting alters plasma and fecal metabolome*

187 We performed nuclear magnetic resonance (NMR) spectroscopy on plasma and fecal
188 samples to assess the impact of fasting, and its associated microbiome shifts on the fecal and
189 host metabolome. Principal coordinate analysis (PCA), centered on baseline values to
190 characterize post-fast changes and on post-fast values to characterize follow-up effects,
191 revealed plasma metabolome trajectories analogous to those observed in the gut
192 microbiome (Figure S4b). In line, we observed significant alterations between baseline,
193 fasting, and follow-up, with most changes reversed at follow-up (Figure S4c, Supplementary
194 Data 4). In plasma, only valine, glycine, tyrosine, and pyruvic acid exhibited sustained
195 increases from baseline to follow-up, indicating lasting effects of fasting on these metabolites
196 (Figure S4b, c).

197 Fecal metabolite profiling again revealed a pattern of alteration and reversion to baseline
198 (Figure S4d). Contradicting other previous reports on short-chain fatty acids (SCFA) in
199 fasting[5], we observed a decrease in butyrate during fasting, which was non-significant at
200 follow-up (Figure S4e, Supplementary Data 5). The only long-term effect observed in our data
201 was a decrease in choline from baseline to fasting (Figure S4e).

202 In conclusion, NMR-based metabolomics of plasma shows more consistent alterations as
203 compared to the fecal metabolome, which might be due to the different matrix or
204 intraindividual variations in gut microbiome composition.

205

206 *Prediction of sustained BMI response by multi-omics machine learning*

207 Since we observed strong intraindividual differences in response to prolonged fasting across
208 most data layers, we aimed to investigate whether the clinical response to fasting can be
209 predicted from baseline data. BMI showed the overall strongest long-term effect of the

210 analyzed clinical data (Figure 1). Therefore, we focused on the long-term weight loss
211 response as the primary phenotype that we aimed to predict. Using the waiting list control,
212 we estimated the normal fluctuation of BMI within 12 weeks of study participation. Normal
213 fluctuation in BMI was defined as mean ± two standard deviations (SD)[21], in our case -0.008 ±
214 0.32 kg/m^2. Based on this threshold, we identified 38% long-term responders and 62% non-
215 responders to prolonged fasting.
216 To predict BMI loss response, a random forest classifier was trained on 87 features including
217 the 50 most abundant microbial species at baseline, additional candidate taxa and pathways
218 from previous prolonged fasting studies, and relevant clinical metadata (Supplementary Data
219 6). To obtain a model that would be as transferable as possible to publicly available datasets,
220 we focused on microbiome and clinical features rather than NMR metabolomics[5,22]. Due to
221 the small sample size, we applied a repeated cross-validation approach to ensure robust
222 model evaluation. Specifically, we used 100 repeated stratified 80/20 resamples, each
223 incorporating an inner 5-fold cross-validation loop for hyperparameter tuning. Model
224 performance was further optimized by performing feature selection once after model tuning,
225 based on random-forest feature importance, the Boruta algorithm, and backward feature
226 elimination (Figure 3b, S5c). This resulted in four features: LDL, systolic blood pressure (BP),
227 *Faecalibacterium sp.* incerta sedis and *Oscillibacter sp.* 57_20. Those four features were used
228 to train the final model. Across the repeated 80/20 resampling, the refined short model
229 performed well with an AUC of 0.84 ± 0.17 (Table 2).
230 Baseline BMI can confound weight loss prediction. Therefore, we tested collinearity between
231 baseline BMI and our four selected features, none of which reached significance (Figure 3c).
232 To test if the four selected features are mere surrogate markers of baseline BMI, we
233 incorporated baseline BMI into the model. This did not improve predictive accuracy (Figure

234 S5b). Furthermore, *Oscillibacter sp.* 57_20 remained the most important feature. Feature-
235 stability analysis supported this ranking: *Oscillibacter sp.* 57_20 and *Faecalibacterium sp.*
236 incertae sedis consistently ranked highest, followed by systolic BP, while LDL showed low and
237 inconsistent importance (−0.9 ± 3.2; Supplementary Table S2a). To avoid post-hoc feature
238 removal, LDL was retained in the sparse model, although a 3-feature variant performed
239 similarly (Supplementary Table S3). Next, we compared a clinical-only model (including
240 baseline BMI, blood pressure, and lipid parameters) with a combined model that additionally
241 incorporated microbiome data to address potential confounding by clinical features (Table 3).
242 The clinical-only model achieved an AUC = 0.69 ± 0.21, accuracy = 0.66 ± 0.18, and balanced
243 accuracy = 0.62 ± 0.19 (Table 3). The combined model improved performance across all
244 metrics (AUC = 0.86 ± 0.17, accuracy = 0.74 ± 0.16, balanced accuracy = 0.72 ± 0.18, Table 3).
245 These results indicate that microbiome features contribute predictive information beyond
246 standard clinical covariates, underscoring their added value for identifying responders to
247 prolonged fasting.
248 Finally, we examined the abundance patterns of the four features from the reduced model
249 within our cohort. Responders exhibited significantly higher levels of *Oscillibacter sp.* 57_20
250 (Figure 3d), while the identified *Faecalibacterium sp.* showed no significant difference (Figure
251 3f). Although systolic BP and LDL contributed to model classification, their individual baseline
252 levels did not differ significantly between responders and non-responders (Figure 3e, g).
253 Taken together, we identified four (two clinical and two microbiome) features that jointly
254 hold the potential to predict long-term weight loss in response to prolonged fasting
255 intervention. Although performance remained consistently above random across repeated
256 cross-validation, we emphasize the expected variability due to small cohort size and interpret
257 the findings as exploratory but reproducible evidence of predictive potential.

258

259 *Application of the classifier in independent cohorts*

260 To test transferability in independent datasets, we applied the final model to data from three
261 publicly available cohorts that differed in health status and fasting design. Given these
262 differences, these analyses are treated as exploratory applications rather than formal
263 external validations.

264 As a first step, we applied our model to our published metabolic syndrome cohort, in which
265 patients underwent either a five-day fasting regimen followed by a DASH diet or a DASH diet
266 alone (Figure 4a, n=34)[5]. The study outcomes were assessed 12 weeks post-intervention,
267 mirroring our study's timeline. Given the greater BMI variability expected in metabolic
268 syndrome patients, we quantified BMI fluctuation from the DASH only group (control group).
269 Long-term responders were again defined as exceeding the mean plus two standard
270 deviation weight loss of the control group (DASH only), corresponding to BMI reduction
271 exceeding 0.8 kg/m^2. Remarkably, our trained model predicted sustained weight loss in this
272 study with an AUC of 0.85 (Figure 4b-c, Supplementary Table S3). Next, we calibrated the
273 model using Platt scaling and isotonic regression. Despite stable strong discrimination, the
274 Brier score remained unchanged after calibration (Supplementary Table S3), indicating that
275 residual error likely reflects differences in outcome prevalence or underlying data
276 distributions rather than miscalibration alone. Consistent with our healthy-participant
277 cohort, the model's predictive features exhibited only weak correlations with baseline BMI,
278 underscoring their independence from initial body mass (Fig. 4d). In univariate analyses,
279 *Oscillibacter sp.* 50_27 and *Faecalibacterium sp.* showed significant differences at baseline
280 between responders and non-responders, while clinical features showed no
281 difference (Figure 4e-h).

282 As a further dataset, we applied the classifier to a recent nutritional intervention trial in
283 patients with multiple sclerosis, the majority of whom exhibited normal metabolic profiles
284 (obesity in one patient, hypertension in two, and elevated LDL in four)[22]. Notably, the study
285 design differed from the other cohorts. Patients completed two prolonged 7-day periods of
286 fasting (Figure 5a, n=22). However, these prolonged fasting periods were interspersed with
287 intermittent fasting (14 hrs/ day), and follow-up assessments were conducted nine months
288 apart (Figure 6a). Because no control arm was available to isolate the effects of the
289 prolonged fasting periods from those of intermittent fasting, we could not define average
290 BMI variation and thus compute specificity and sensitivity or perform calibration. However,
291 patients classified as responders by our model experienced significantly greater weight loss
292 than those classified as non-responders (Figure 5b). To provide an alternative quantitative
293 assessment, we evaluated the correlation between the probability of responder classification
294 and the observed magnitude of BMI change (Figure 5c). While the Spearman correlation did
295 not achieve statistical significance ($p=0.08$), the direction and magnitude of the association
296 ($\rho=0.309$) support the model's ability to reflect observed BMI changes. No significant
297 correlations between model parameters and baseline BMI were detected (Figure 5d). Similar
298 to the current cohort, levels of *Oscillibacter sp.* 50_27 were significantly higher in responders
299 (Figure 5e), while the other features did not differ significantly (Figure 5f-h).
300 Lastly, we applied the model to available data from healthy volunteers undergoing between 6
301 and 12 days of prolonged fasting[23]. This dataset comprises two subcohorts: the GENESIS
302 (ClinicalTrials.gov: NCT05449249) and OralFast (ClinicalTrials.gov: NCT05031598) trials. Both
303 follow similar study designs (Figure 6a) but differ in their follow-up durations — 3 months for
304 OralFast and 4 months for GENESIS. Outcome was assessed after 16 weeks during a study
305 visit and as self-reported outcome after 12 weeks, respectively (Figure 6a, n=47). Since this

306 study was performed in healthy participants, we used the same BMI cut-offs for responder
307 definition as used for the model training in our cohort. Our trained model predicted
308 sustained weight loss in this study with an AUC of 0.655. (Figure 6b-c, Supplementary Table
309 S4). Of note, AUC was slightly better for the GENESIS than the OralFast data (Figure 6b). Platt
310 scaling and isotonic regression did not improve model calibration but retained consistent
311 discrimination (Supplementary Table S4). In contrast to the other cohorts, baseline BMI and
312 systolic blood pressure were correlated (Fig. 6d). In univariate analyses, none of the features
313 differed significantly at baseline between responders and non-responders (Figure 6e h).
314 Our findings indicate that baseline patient characteristics determine the magnitude of long-
315 term weight response to prolonged fasting interventions. Furthermore, the predictive model,
316 initially developed in healthy subjects, was successfully applied to independent cohorts
317 investigating prolonged fasting. However, given the differences in health status, study design,
318 and the absence of an intermittent fasting-only group in the multiple sclerosis cohort, this
319 represents an exploratory rather than a formal validation. The observed association between
320 predicted responder status and actual BMI reduction provides supportive but not
321 confirmatory evidence of external applicability, highlighting the need for larger, harmonized
322 fasting studies to confirm generalizability.
323
324 *Metabolite associations with Oscillibacter sp.* 57_20 *and Faecalibacterium sp.* incertae sedis
325 Since both the *Oscillibacter sp.* 57_20 and the *Faecalibacterium sp.* identified in the LEANER
326 were predictive of weight loss, we wanted to further understand the potential metabolite
327 profile associated with these bacteria. Therefore, we performed an exploratory correlation
328 analysis with the fecal metabolome across all visit data while blocking the visit information[24].
329 We found significant associations of *Faecalibacterium sp.* with butyrate, tryptophan, and

330 uridine (Figure 7a-c, Supplementary Data 7) as well as of *Oscillibacter sp.* 57_20 with glycerol
331 and methionine, and for uridine without reaching statistical significance (Figure 7d-f,
332 Supplementary Data 8). In summary, our data suggests that the bacterial species important
333 for the classification of long-term body weight responders modulate the metabolomic output
334 of the fecal microbiome.

335 **Discussion**

336 Our data show that prolonged fasting leads to long-term body weight and body fat reduction
337 after 12 weeks. Interindividual variability in response to dietary interventions poses a major
338 challenge in lifestyle interventions. Large-scale studies have shown that both host and
339 microbial factors shape individual metabolic responses, emphasizing the need for precision
340 strategies[25,26]. Using baseline microbiome and clinical data, we can predict individuals who
341 will respond to fasting with sustained weight loss, defined as a BMI reduction lower than the
342 mean minus two standard deviations of the waiting list control. Using available data from
343 similar interventions in healthy volunteers, patients with metabolic syndrome, and patients
344 with multiple sclerosis, we could apply our data-driven classification approach. While
345 *Faecalibacterium sp.* incertae sedis and *Oscillibacter sp.* 57_20, were important for BMI
346 response prediction, most of the microbiome and metabolome features were characterized
347 by transient shifts induced by fasting, with subsequent return to pre-intervention states.
348 Taken together, our data implicate gut microbiota in long-term BMI changes post fasting and
349 suggest conserved effects of fasting regardless of health status. We used a data-driven
350 definition of responders, defining weight loss beyond the mean plus two standard deviations
351 of the control group in each cohort (the waiting-list control in the current study and the
352 DASH-only arm in the Maifeld et al. cohort). This represents a statistical rather than a clinical
353 threshold, chosen to capture changes exceeding normal physiological variation[21]. While this
354 approach ensures objectivity across cohorts, it may not fully reflect clinically meaningful
355 improvements, which future studies with larger and harmonized samples should define more
356 precisely.

357 On the host level, prolonged fasting led to strong changes in multiple cardiometabolic risk
358 factors like LDL cholesterol, waist-to-hip ratio, and systolic and diastolic blood pressure.

359 However, at the 12-week follow-up these changes had mostly reverted, indicating that
360 prolonged fasting did not exert a sustained effect in healthy individuals. These data differ
361 from patients with metabolic syndrome with values above the healthy range[5]. Interestingly,
362 while blood glucose dropped during fasting, it increased upon refeeding during the day (6am
363 to 10pm). Since values at night (10pm to 6am) did not increase, our data suggest a mildly
364 disturbed glucose handling for the early days post-fasting. A similar phenotype was reported
365 in the literature in response to standardized meal intakes after prolonged fasting[27,28]. This
366 was attributed to the metabolism successfully switching to fatty acid and ketone oxidation
367 and postprandial carbohydrate oxidation was reduced, leading to higher plasma glucose
368 levels[27]. Since a strong metabolic phenotype was expected, REE reduction was our
369 predefined endpoint. REE in fasting was studied previously mainly in healthy men[29-31]. Our
370 data shows an overall similar but smaller effect, which might be due to the inclusion of
371 healthy women and a broader range of lean masses. REE reduction after 24h caloric
372 deprivation was previously associated with weight gain after 6 months in healthy
373 individuals[32]. We could not confirm these findings in our cohort for long-term weight
374 changes after 3 months using the changes in REE after 5 days of fasting (Figure S6). However,
375 using a combination of clinical and microbiome data, we were successful in predicting long-
376 term weight loss.
377 We have shown in the past the microbiome and immune data can predict blood pressure
378 reduction in patients with metabolic syndrome in response to fasting[5]. In contrast, our study
379 in healthy participants revealed only modest effects on blood pressure. Given the well-
380 established impact of fasting on weight management[33], we applied a data-driven approach
381 that involved clustering participants based on BMI changes and employing a random forest
382 classifier. Our initial model, which incorporated 83 features, demonstrated high sensitivity

383 but limited specificity. Iterative feature selection enabled us to identify *Faecalibacterium sp.*
384 incertae sedis, *Oscillibacter sp*. 57_20, plasma LDL levels, and systolic blood pressure for a
385 feature-reduced classifier. Notably, the successful application of the model in independent
386 cohorts highlighted the robustness and generalizability of our approach. In the Maifeld et al.
387 cohort[5], which featured a similar study design in patients with metabolic syndrome, we
388 observed an 82.6% of responders were correctly identified. In the Bahr et al. cohort[22], with a
389 different study design incorporating intermittent fasting in patients with multiple sclerosis,
390 predicted responders exhibited higher weight loss. Furthermore, we tested the model in a
391 cohort of healthy volunteers published by Ducarmon et al.[23]. In this cohort, discrimination
392 was moderate (AUC = 0.655), which we interpret as evidence of partial but attenuated signal
393 transfer. Several methodological and biological factors likely contributed to this reduction in
394 performance. First, the follow-up timing at 3 months for one subcohort and 4 months for the
395 other differed from the standardized 12-week follow-up applied in both our primary study
396 and the Maifeld et al. cohort. The longer interval increases the influence of post-intervention
397 behavior, which weakens the link between baseline microbiota and long-term weight
398 dynamics. Second, outcomes in the OralFast subcohort were self-reported rather than
399 measured, introducing non-differential measurement error and potential bias. Self-reported
400 weight is known to systematically underestimate true body weight change, particularly in
401 non-obese individuals[34], and such noise disproportionately affects probabilistic classifiers by
402 compressing the outcome distribution. Third, the fasting protocol in Ducarmon et al. involved
403 substantially deeper caloric restriction than the 5-day intervention used in our study. Longer
404 fasting typically produces a larger initial weight loss driven by acute depletion of glycogen
405 stores and associated water and lean mass changes[35], thereby diluting the proportion of
406 weight loss attributable to microbiota-dependent mechanisms. Furthermore, the fasting

407 duration in itself was heterogenous among participants (6-12 days) and not standardized to a
408 certain number of days[5,22]. Finally, the physiological measurements across the studies were
409 not fully harmonized. Blood pressure, a feature that contributes to the clinical context of the
410 model, was assessed in our study and in the Maifeld and Bahr cohorts using a standardized
411 protocol with an oscillometric device (Mobil-O-Graph)[5,22]. In contrast, Ducarmon et al.[23],
412 used a different measurement approach, which may introduce variability in clinical
413 covariates relative to the trained model. Notably, in this dataset, baseline BMI and systolic
414 blood pressure were correlated, unlike in the other cohorts, suggesting population-specific
415 interactions between anthropometric and cardiovascular traits that were not present during
416 model training.
417 Taken together, these differences in study design, outcome measurement, physiological
418 assessment, and fasting intensity likely account for the attenuated but still meaningful
419 predictive performance in the Ducarmon dataset. The moderate AUC indicates that the
420 classifier captures a biological signal that remains detectable across heterogeneous fasting
421 contexts, but that true external validation will require cohorts with harmonized protocols,
422 standardized follow-up durations, and objectively measured outcomes.
423 To assess whether calibration could improve probability estimates, we applied post-hoc
424 calibration using Platt scaling and isotonic regression. However, these adjustments enhanced
425 predictive performance in neither of the two external datasets. Post-hoc calibration often
426 fails when the underlying problem is a mismatch between the training and validation cohorts
427 rather than statistical miscalibration[36]. In our case, differences in fasting protocol, follow-up
428 period, and even methodological aspects such as systolic blood pressure measurement, as
429 mentioned above, likely contributed to the reduced model transferability. Calibration
430 methods can only improve prediction when the target data share similar distributions and

431 measurement contexts with the training data; they cannot correct for biological, behavioral,
432 or procedural heterogeneity[37]. In contrast, the Maifeld et al. cohort demonstrated robust
433 discrimination, but most likely the limited sample size constrained formal calibration.
434 Together, these findings highlight that while our model retains general discriminative
435 capacity across independent datasets, its probabilistic calibration and transportability
436 depend on harmonized study protocols and consistent data collection practices.
437 These external explorations not only reinforce the reliability of our predictive model but also
438 suggest that the gut microbiome changes associated with fasting responses are conserved
439 across diverse populations, from healthy individuals to those with metabolic disorders and
440 autoimmune disease, thereby broadening the potential applicability of fasting-based
441 interventions for weight management and metabolic health.
442 An important aspect of our findings is the distinction between the multivariate classifier and
443 univariate analyses of individual features. While none of the selected predictors were
444 consistently significant when tested individually, their combined predictive value was clearly
445 demonstrated by the random forest classifier[38]. This reflects the interdependent nature of
446 biological systems, where linear and nonlinear relationships among variables often provide
447 stronger discriminative power than single-feature associations[39]. However, univariate
448 analyses remain valuable for hypothesis generation and mechanistic interpretation, as
449 performed extensively across cohorts to contextualize individual predictors[39]. This pattern
450 has also been observed in previous microbiome-based prediction studies, where integrative
451 models outperform single-feature analyses by capturing interdependent microbial and host
452 effects[40].
453 At the same time, we recognize that differences in underlying disease, medication use, and
454 dietary context across cohorts may confound microbiome–BMI associations and limit direct

455 transferability of model coefficients[41]. The relatively small sample size of the training cohort
456 adds further uncertainty, although consistent results in three independent datasets support
457 the robustness of our approach. Therefore, the present model should be viewed as
458 exploratory evidence that microbiome and clinical features together contain predictive
459 information for fasting responses, rather than as definitive proof of generalizable biomarkers.
460 Future validation in larger, prospectively harmonized fasting cohorts will be essential to
461 confirm the robustness and clinical utility of these predictors.
462 Given that baseline BMI is typically a predictor of weight loss, we assessed its confounding
463 effect on fasting-induced BMI changes. *Oscillibacter sp.* 57_20 remained the stronger
464 predictor even when baseline BMI was included in the model, indicating that this microbial
465 species may exert an independent influence on weight regulation during fasting. While we
466 cannot fully exclude potential confounding or correlations between baseline BMI and
467 microbiome composition, to our knowledge, no prior study has directly linked *Oscillibacter*
468 *sp.* 57_20 with weight regulation. However, *Oscillibacter sp.* 57_20 was recently identified as
469 a keystone taxon in a similar prolonged fasting study in healthy individuals, where it was
470 implicated in the production of indole-3-propionate (I3P)[23], a protective metabolite in
471 cardiometabolic disease[42]. Future research is needed to explore the mechanistic role of
472 *Oscillibacter spp.* in host metabolism and its potential relevance in personalized fasting
473 interventions.
474 *Faecalibacterium spp.* are known SCFA producers[43]. In line, our data shows that the
475 abundance of our specific *Faecalibacterium sp.* associates with fecal butyrate levels. As
476 described previously for other *Faecalibacterium spp.*[44], the identified *Faecalibacterium sp.*
477 correlates with fecal tryptophan. Tryptophan can be catabolized by gut microbiota to indole
478 metabolites[45]. Unfortunately, due to the resolution of NMR metabolomics, we could not

479 detect specific indole metabolites like I3P. However, our data imply that both bacteria might
480 interact in the production of tryptophan catabolites.
481 Both the *Faecalibacterium sp.* identified in this study and the *Oscillibacter sp.* 57_20
482 correlate with the nucleoside uridine. Uridine can adaptively regulate food intake in healthy
483 participants[46]. Furthermore, experimental evidence show that blood uridine levels reflect the
484 nutritional status of mice[47,48] with high uridine levels as indicators of catabolic states[47,49]. In
485 line, dietary supplementation of uridine enhanced hunger and increased caloric intake[46].
486 Microbial metabolism of uridine suggests a potential role of a gut-brain axis or influence on
487 satiety[50] in long-term BMI responders. Unfortunately, the literature concerning the other
488 metabolites of interest correlating with *Oscillibacter sp.* 57_20, glycerol and methionine is
489 sparse. While we controlled our analysis for abundance shifts at different visits, we could not
490 control the false discovery rate in this exploratory setting. Future confirmatory studies are
491 needed to further investigate the metabolite spectra of the identified *Faecalibacterium sp.*
492 and *Oscillibacter sp.* 57_20.
493 Overall, the gut microbiome and metabolome exhibited a consistent pattern of fasting-
494 induced alterations and nearly complete reversion to baseline at follow-up. Previous studies
495 have consistently reported an enrichment of beneficial bacteria such as *F. prausnitzii* [51-53], as
496 well as *Roseburia* and *Coprococcus* species, other known SCFA producers[54-56]. Our data only
497 partly overlaps with these reports, as we observed no alterations to *F. prausnitzii*, alongside a
498 decrease in *Roseburia sp.* and *Coprococcus sp.* However, we observed an increase in one
499 *Butyricicoccus sp.,* known butyrate producers. Our functional analysis revealed an increase in
500 propionate production via kinase pathways, pointing towards an elevated SCFA production
501 potential from coordinated activity across a broader microbial community rather than single
502 species effects. The discrepancy with previous findings may be attributed to our study's

503 healthy cohort, in which baseline levels of *F. prausnitzii* are likely already well-balanced. This
504 suggests that fasting might predominantly restore disturbed bacterial populations rather
505 than altering already stable communities.[57] Interestingly and consistent with previous
506 studies, we did not observe an overall change in alpha diversity[5,55]. However, participants
507 with lower baseline alpha diversity responded with a long-lasting increase to the fasting
508 intervention. High microbial diversity stabilizes microbiota functions during perturbations[58].
509 In diseases usually associated with lower alpha diversity, such as obesity, other fasting
510 interventions increase alpha diversity[59]. Together, these studies reinforce the hypothesis that
511 fasting effects on alpha diversity are more pronounced in individuals with a reduced
512 microbial diversity. However, low baseline alpha diversity may also arise from unaccounted
513 external influences (e.g., lifestyle habits immediately preceding the measurement).
514 Despite these promising results, our study has several limitations. First, the lack of
515 comprehensive documentation on dietary intake following the fasting intervention. Whether
516 significant weight loss was solely due to fasting or also influenced by subsequent dietary
517 modifications, a common limitation in caloric restriction studies cannot be determined. From
518 a computational perspective, the relatively small sample size, particularly the initial test
519 dataset after splitting, poses challenges for the random forest model and feature selection[60].
520 However, the testing of the classifier in three independent cohorts shows the robustness of
521 our approach[61].
522 In conclusion, our study provides compelling evidence that fasting induces substantial yet
523 reversible changes in the gut microbiome and host metabolic profiles. Importantly, a subset
524 of individuals experiences sustained weight loss. The integration of microbial and clinical
525 data not only enhanced our predictive capabilities but also unveiled novel associations, such
526 as the independent role of *Oscillibacter sp.* 57_20 and *Faecalibacterium sp.* incertae sedis in

527 weight regulation. Despite limitations related to dietary documentation and sample size,
528 these findings pave the way for future research aimed at refining personalized fasting
529 interventions. Ultimately, our work underscores the promise of leveraging gut microbiome
530 insights to tailor dietary strategies for improved metabolic health and weight management.

531 **Methods**

532 **Study design**

533 We performed a randomized, waitlist-controlled study (LEANER study, ClinicalTrials.gov;
534 NCT04452916) carried out at the Experimental and Clinical Research Center of Charité –
535 Universitätsmedizin in Berlin, from November 2020 to December 2022. The study protocol
536 was approved by the institutional review board of Charité – Universitätsmedizin Berlin
537 (EA1/033/20) and all participants provided written informed consent before entering the
538 study. We collected and managed study data using REDCap electronic data capture tools
539 hosted at Charité – Universitätsmedizin Berlin[62,63]. This study was exploratory, and we did not
540 calculate a pre-determined sample size. Instead, the size of the recruited cohort was
541 determined based on methodological and feasibility considerations. Flow diagram of
542 recruitment and enrollment of patients according to Consort 2025 guidelines[64] is shown in
543 Figure S7. A general overview of the study is provided in Fig. 1a.

544

545 **Eligibility criteria**

546 We included individuals aged 20-50 years who were assigned male or female at birth and
547 identified as men and women, respectively; with a body mass index between 20-30 kg/m^2.
548 Exclusion criteria were heart, lung, liver, and kidney diseases requiring medical intervention,
549 prescribed medication (except oral contraceptives), postoperative phases, current or chronic
550 infection, antibiotic treatment or a fasting week within the last 6 months, habitual use of
551 dietary supplements, food intolerances, > 2 kg body weight change within the last month,
552 pregnancy, lactation, vegan diet, smoking, drug, or alcohol abuse.

553

554 **Intervention**

555 Participants received oral and written instructions on the method of prolonged fasting.
556 Expert guidance was provided by experienced nutritionists and certified fasting counselors in
557 a group setting with 5-10 participants per group. After sufficient instruction, the fasting was
558 performed individually at home, with the possibility of reaching out to the counselor at any
559 time or to connect with other group members (if patients gave consent to share this
560 information). Participants were encouraged but not required to take time off during this
561 week. Fasting was preceded by one preparation day, on which participants consumed a low-
562 calorie, fiber-rich diet, e.g. fruits, vegetables, potatoes, rice, and oats.
563 During the five fasting days, participants were allowed to consume 200-250 kcal/d through
564 vegetable juices and vegetable broths. Herbal teas and water could be consumed ad libitum.
565 At the morning of fasting day 6, we performed the study visit and patients were instructed
566 for the refeeding phase. A detailed fasting plan including refeeding recommendation is
567 provided as Supplementary Table S6.
568
569 **Randomization**
570 We assigned participants randomly according to a locked list created by www.randomizer.at
571 (two treatments: waiting, fasting; 1 factor: self-reported sex; permuted blocks; block sizes 4,
572 2, 6, 4). Due to the nature of the intervention and the wait-list design, blinding was not
573 possible.
574
575 **Outcome measures**
576 We established all outcome measures in advance and did not adapt them during or after the
577 study. The primary outcome measure was resting energy expenditure (REE in kcal/d) after 5
578 days of fasting vs. baseline 1 assessed by indirect calorimetry. Secondary outcomes were

579 body composition, cardiovascular parameters, various routine blood parameters, glucose
580 variability, gut metagenome, fecal, and plasma metabolome. In addition, we assessed
581 compliance and safety of fasting.
582
583 **Study center assessments**
584 The waiting group underwent assessments four times, the fasting group three times. The
585 fasting group had one baseline visit (baseline 1) and started the intervention within two to
586 eleven days afterwards, the waiting group had two baseline visits with a 12-week waiting
587 period in between (baseline 0 and baseline 1) and also started the intervention within a
588 maximum of 11 days after baseline 1. These two baselines allowed detection of random time
589 effects on the assessed outcome measures. For both groups, the next visit was on the
590 morning of the sixth fasting day directly before breaking the fast (fasting). To assess medium-
591 term effects of fasting, there was another visit after 12 weeks (follow-up). Except for the
592 additional baseline 0 in the waiting group, all assessments were identical between the
593 groups. All examinations described hereafter were performed at all study visits.
594 Assessments commenced in the morning following a 12-hour overnight fast. Participants
595 were instructed to abstain from caffeine, alcohol, and vigorous exercise for 24 hours prior to
596 the assessments.
597 Venous blood was drawn and sent to an accredited laboratory (Labor Berlin, Berlin,
598 Germany) that measured parameters of glucose and lipid metabolism, blood count,
599 electrolytes, liver enzymes, uric acid, CRP, and renal function according to international
600 standards.

601 We measured waist and hip circumference to calculate waist-to-hip ratio and determined
602 body composition (lean and fat mass) by air displacement plethysmography (Bod Pod, Life
603 Measurements, Inc., Concord, CA).
604 Indirect calorimetry was conducted following a 30 min resting period while in a supine
605 position within a thermoneutral environment for a duration of 30 min (Quark RMR, COSMED,
606 Italy). REE and respiratory exchange ratio (RER) were calculated from oxygen consumption
607 and carbon dioxide production as described elsewhere.[65]
608 Office blood pressure and heart rate were determined by five automated measurements
609 within 10 min with an upper arm cuff (Mobil-o-Graph, I.E.M. GmbH, Stolberg, Germany) in
610 the absence of study personnel.
611
612 **Fecal samples**
613 At each study visit, participants received two stool collection kits and were asked to collect
614 two samples from one stool at home as soon as possible following the study visit. One
615 sample was used for gut metagenome sequencing (OMNIgene Gut, DNA Genotek, Ottawa,
616 Canada) and the other for metabolome analysis (OMNImet Gut, DNA Genotek, Ottawa,
617 Canada). These kits allow shipment without cooling to the study center. Participants sent the
618 tubes to the study center at room temperature, where they were stored at - 80°C until
619 further processing.
620
621 **Glucose sensors**
622 We assessed glucose variability by continuous glucose monitoring over 14 days. For this,
623 participants wore a glucose sensor that measured interstitial glucose concentrations in the
624 subcutaneous tissue of the dorsal upper arm every 15 min (FreeStyle Libre Pro, Abbott,

625 Chicago, IL, USA). In contrast to the use of these sensors in diabetic patients, participants in
626 this study could not see their values during the measurement. Baseline assessment was done
627 only in the waiting group directly following baseline visit 0. Additionally, fasting assessment
628 was done in all participants during preparation, fasting, and refeeding.
629
630 **Ketone and glucose measurements**
631 On the five fasting days, participants independently measured their blood concentration of
632 beta-hydroxybutyrate (BHB) and glucose twice daily using a handheld glucometer (Freestyle
633 Precision Neo, Abbott, Chicago, IL, USA), and recorded their values in a provided protocol. In
634 addition, values were stored on the device and read out later in the study center, providing
635 an objective measure of compliance.
636
637 **Fecal metagenomic sequencing**
638 *DNA isolation*
639 DNA was isolated using ZymoBIOMICS DNA Miniprep Kit (ZymoReseach Europe GmbH,
640 Freiburg, Germany). In short, an aliquot of 250 µL of stool sample from the OMNIgene Gut
641 tube was added to a ZR BashingBead Lysis Tube. The following extraction was done according
642 to the manufacturer's instructions. DNA was eluted in 100 µL RNase/DNase-free water and
643 collected in a 1.5-mL Eppendorf tube. Total DNA concentration was measured using
644 NanoDrop ND-1000 (Peqlab Biotechnologie GmbH, Erlangen, Germany). Isolated DNA was
645 stored at
646 -80°C[66].
647
648 *Shotgun metagenomics*

649 Isolated DNA was shipped on dry ice to Novogene (Cambridge, UK) for shotgun metagenomic
650 DNA sequencing. In short, DNA was fragmented and subsequently underwent end repair and
651 phosphorylation. After A-tailing, adapter ligation was performed. Then 150 bp paired-end
652 sequencing was performed on the Illumina Novaseq 6000 platform with an aimed data
653 collection of 6Gb raw data.
654
655 *Microbiome data processing*
656 Sequencing reads were mapped to the mOTUv2 (version 2.6) database, and read counts
657 were subsequently rarefied using the RTK R package (version 0.2.6.1) to standardize
658 sequencing depth across samples. Rarefaction involves randomly subsampling reads to
659 match the sample with the lowest read depth, thereby mitigating biases introduced by
660 variable sequencing depth and enabling reliable comparisons across cohorts. For the LEANER
661 (healthy) cohort, a cutoff of 3,859 reads was applied, resulting in the exclusion of one sample
662 due to insufficient sequencing depth. The same threshold was used for the Maifeld cohort[5],
663 where one sample was also excluded. In the Bahr dataset[22], applying the same rarefaction
664 criteria led to the exclusion of one sample. In the Ducarmon dataset[23], applying the
665 consistent rarefaction criteria resulted in the exclusion of 9 baseline samples (7 from GENESIS
666 and 2 from OralFast trial). This consistent approach enabled reliable comparisons across
667 cohorts and increased the robustness of downstream analyses.
668
669 **Plasma metabolomics**
670 *Collection of plasma*

671 Venous blood was collected in Vacutainer® EDTA tubes (BD, Heidelberg, Germany) and
672 immediately put on crushed ice for 30 min and then centrifuged (3,000 x g, 4°C, 10 min).
673 Plasma was collected and stored at - 80°C.
674
675 *Preparation of plasma for nuclear magnetic resonance spectroscopy (NMR)*
676 Plasma samples were prepared with a robotic system (SamplePro Tube, Bruker BioSpin
677 GmbH, Ettlingen, Germany) by mixing 287 µL plasma with 287 µL IVDr buffer (Bruker BioSpin
678 GmbH, Ettlingen, Germany) and adding 10 µL formic acid (240 mM) as internal standard.
679
680 *NMR measurement of plasma*
681 All NMR experiments were performed on a 600 MHz Bruker Avance III spectrometer, using a
682 triple resonance (^{1}H, ^{13}C, ^{15}N, ^{2}H lock) helium cooled cryoprobe with z-gradient. Samples
683 were handled by an automatic Bruker SampleJet sample changer (Bruker Biospin GmbH,
684 Ettlingen, Germany). Tuning and matching of the probe as well as locking and shimming of
685 the sample were performed automatically. Following the Bruker IVDr protocol for plasma
686 measurements for each sample, four different types of ^{1}H NMR spectra were acquired at 310
687 K (1D NOESY, 2D JRES, 1D CPMG, and 1D spin echo diffusion spectrum).
688
689 *Data analysis of plasma NMR spectra*
690 From the collected spectra of each specimen, 41 smaller, non-lipoprotein metabolites were
691 automatically identified and quantified using the Bruker IVDr Quantification in Plasma/Serum
692 B.I.Quant-PSTM platform. Of note, only metabolites levels not bound to proteins were
693 determined. Additionally, 112 lipoprotein parameters including various lipoprotein fractions,

694 classes and subfractions were identified and quantified using the Bruker IVDr Lipoprotein
695 Subclass Analysis B.I.LISATM platform.
696
697 **Stool metabolomics**
698 *Drying of stool samples*
699 Fecal samples from OMNImet Gut tubes were processed for metabolomics. Fecal samples (1
700 mL) were dissociated two times after adding 2.5 mL 70% isopropanol using C tubes with the
701 gentleMACS OctoDissociator (Miltenyi Biotec, Bergisch Gladbach, Germany). Aliquots of
702 dissociated samples were covered with perforated Parafilm and dried overnight in a vacuum
703 concentrator (Concentrator 5301, Eppendorf, Hamburg, Germany). Dried samples were
704 stored at - 80°C.
705
706 *Preparation of stool for NMR*
707 Dried stool samples were resuspended in 600 µL (< 10 mg dry weight), 800 µL (10-40 mg dry
708 weight) or 1,000 µL (> 40 mg dry weight) of double distilled water and 10 µL of an extraction
709 standard (Nicotinic acid at 80 mmol/L) were added. Samples were centrifuged three times
710 (12 000 x g, 4 °C, 10 min) and supernatants were transferred into a fresh vial after each
711 centrifugation to remove particles. Of the final supernatant, 400 µL were mixed with 200 µL
712 of 0.1 mol/L phosphate buffer (pH 7.4) and 50 µL of a 0.75% (w/v) solution of 3-
713 trimethylsilyl-2,2,3,3-tetradeuteropropionate (TSP; Sigma-Aldrich, Taufkirchen, Germany),
714 which served as an internal standard, in deuterium oxide.
715
716 *NMR measurements of stool*

717 NMR experiments were conducted on the same NMR spectrometer as described for the
718 plasma analyses. Before measurement, each sample was allowed to equilibrate for 300 sec in
719 the magnet, and the probe was automatically locked, tuned, matched, and shimmed. One-
720 dimensional ^{1}H NMR spectra were obtained at 298 K using a nuclear Overhauser
721 enhancement spectroscopy pulse sequence with solvent signal suppression by pre-saturation
722 during relaxation and mixing time. For each spectrum, 512 scans were collected into 65,536
723 data points over a 20-ppm (parts/million) spectral width using a relaxation delay of 4 sec, an
724 acquisition time of 2.66 sec, and a mixing time of 0.01 sec. Spectra were automatically
725 Fourier transformed and phase and baseline corrected.
726
727 *Data analysis of stool NMR spectra*
728 In each spectrum, a set of 41 metabolites were semi-automatically identified and relative to
729 the TSP reference signal quantified using the CHENOMX 9.02 (Chenomx Inc, Edmonton,
730 Canada) software suite. To account for potential losses during sample preparation, resulting
731 data was adjusted to the extraction standard and normalized to dry weight.
732
733 **Predictive modelling of BMI response**
734 To predict long-term BMI response to prolonged fasting, we used a random forest classifier
735 implemented in the caret package (R 7.0.1). The outcome variable was responder status
736 (responder vs. non-responder) defined by a BMI reduction exceeding the mean plus two
737 standard deviations of the waiting list control group. Predictor variables included either (i)
738 the full set of 87 microbiome and clinical features (Supplementary Data 6) or (ii) a predefined
739 sparse model with four predictors: *Oscillibacter sp.* 57_20, *Faecalibacterium sp.* incertae
740 sedis, systolic blood pressure, and LDL cholesterol. Given the limited sample size (n = 34), we

741 used 100 stratified 80/20 Monte-Carlo resamples with inner 5-fold cross-validation for
742 hyperparameter tuning, using the area under the ROC curve (AUC) as the optimization
743 metric. The best-performing model from each resample was evaluated on its holdout 20%
744 test partition, providing a distribution of performance estimates rather than a single value.
745 Model performance was assessed by AUC, accuracy, sensitivity, specificity, balanced
746 accuracy, F1 score, Matthews correlation coefficient (MCC), and average precision (area
747 under the precision–recall curve). We report both mean ± SD and median [IQR] across
748 resamples to capture variability. Feature importance was obtained via permutation
749 importance, and stability summarized as mean importance ± SD and rank distribution.
750 Feature-stability analysis showed *Oscillibacter sp.* 57_20 and *Faecalibacterium sp.* incertae
751 sedis consistently ranked highest, systolic BP contributed modestly, and LDL showed low and
752 variable importance. LDL was retained in the predefined four-feature model to avoid post-
753 hoc selection, while a three-feature variant performed comparably (Supplementary Table
754 S3).
755 To assess potential confounding and the added predictive value of microbiome data, we
756 trained two additional models using the same resampling procedure: (i) a clinical-only model
757 (age, sex, baseline BMI, blood pressure, lipid parameters), and (ii) a combined model
758 incorporating microbiome predictors.
759
760 **Calibration**
761 To evaluate the reliability of predicted probabilities, we applied post-hoc calibration using
762 Platt scaling (logistic correction of the logit scores) and isotonic regression (monotone, non-
763 parametric mapping) in the Maifeld and Ducarmon cohort. The original model was not
764 retrained. Instead, we performed 100 stratified 80/20 Monte-Carlo resamples, ensuring that

765 both outcome classes were present in each training and test set. For every resample, the
766 calibration models were fit on the training fold only and then applied to the hold-out test
767 fold. We compared three variants of prediction: the raw model (no calibration), Platt-scaled,
768 and isotonic-scaled probabilities.
769 On each test fold, we calculated AUC, accuracy, sensitivity, specificity, balanced accuracy, F1
770 score, Matthews correlation coefficient (MCC), and the Brier score (mean squared error of
771 predicted probabilities). Predictions were dichotomized at a 0.5 threshold to form confusion
772 matrices, summarized as mean ± SD of the test proportion. Calibration was further assessed
773 using Calibration-in-the-Large (CITL) and Calibration Slope in the test fold. All performance
774 measures were summarized as mean ± SD across the 100 repeats.
775
776 **Statistical analysis**
777 Descriptive statistics for interval variables are presented as mean ± standard deviation or
778 median with interquartile range (IQR). For comparisons of delta BMI between responders
779 and non-responders, normality of variable distributions was assessed by visual check of
780 histograms and qq-plots. Mann-Whitney U-test or t-test was used as appropriate. For all
781 other data, comparisons between independent groups were performed using the Mann-
782 Whitney U test, and paired samples were compared using the Wilcoxon signed-rank test.
783 Where applicable, p-values were adjusted for multiple comparisons using either the Holm
784 method (for family-wise error control) or the Benjamini-Hochberg (BH) procedure (for false
785 discovery rate control), depending on the analytical objective.
786 Permutational Multivariate Analysis of Variance (PERMANOVA) was used to test for
787 multivariate compositional differences between groups and visits.

788 To evaluate the relationship between bacterial abundance and metabolite concentrations
789 while accounting for visit timepoint, we performed permutation-based conditional
790 independence tests. Specifically, for each metabolite, its association with *Oscillibacter* sp.
791 57_20 and *Faecalibacterium* sp. incertae sedis was tested while conditioning on the visit
792 variable, using the R package coin (version 1.4.3) with 10,000 permutations. Resulting p-
793 values were corrected for multiple testing using the Benjamini-Hochberg false discovery rate
794 (FDR) method.
795 Statistical significance was defined as $p < 0.05$ or $q < 0.1$, where applicable.

796 **Data and code availability**

797 All code, data, and scripts used in this study have been made publicly available. The code,
798 scripts, and processed raw data can be accessed on Zenodo
799 (doi: https://doi.org/10.5281/zenodo.17493808). Raw sequencing data will be made
800 available under the BioProject ID PRJNA1293883 from the NIH Sequence Read Archive.

801

802 **Acknowledgement**

803 We would like to thank Anja Mähler for designing and setting up the LEANER study, for
804 recruiting the study cohort, the entire study organization, and establishing the network
805 around this fasting study. We thank Alexandra Prüß who assisted as a fasting guide in
806 carrying out study protocols. We thank Jana Czychi for her excellent technical assistance. This
807 work was funded by intramural funds of the Experimental and Clinical Research Center, a
808 cooperation between the Max Delbrück Center for Molecular Medicine in the Helmholtz
809 Association and Charité – Universitätsmedizin Berlin; and external funds from the Karl and
810 Veronica Carstens foundation (KVC 0/120/2021).
811 FP, NW, HB, DNM, WG and PJO were supported by the BMFTR (Federal Ministry of Research,
812 Technology and Space), project IDs 01EJ2202A, 01EJ2202D and 01EJ2202B (TAhRget
813 consortium). FP, NW, and SKF were supported by the European Union (HORIZON-HLTH-2022-
814 STAYHLTH-02, IMMEDIATE consortium). TUPB was supported by the Berlin Center for
815 Translational Vascular Biomedicine, jointly founded by BIH, Charité - Universitätsmedizin, and
816 the Max Delbrück Center. DNM and NW were supported by the DZGIF (DZG Innovation
817 Fund), Topic "Microbiome". SKF, DNM and NW were supported by the German Research
818 Foundation (DFG), project ID 437531118 (CRC1470, projects A05, A06 and A10). SKF was

supported by the DFG project TRR412 and DZHK. AZ was supported by the DFG, project ID 324392634 (TR221).

Author Contributions

CRediT: Conceptualization: TUPB, SB, HB, NS; Data curation: GNK, TUPB, LSB, FG, QRD, GZ, RM, SB, HB; Formal Analysis: GNK, TUPB, UL, MM, AK, HB; Funding acquisition: TUPB, NW, PJO, WG, DNM, SKF, SB, HB, NS; Investigation: KK, TS, SK, GR, VM, LB, LM, LSB, FG, FP, QRD, GZ, RM, SB, NS; Methodology: GNK, TUPB, UL, WG, PJO, SKF, HB; Project administration: SB, HB, NS; Resources: NW, AZ, PJO, WG, DNM, SKF, SB, HB, NS; Software: GNK, TUPB, UL, AK, SKF; Supervision: TUPB, UL, AZ, PJO, WG, DNM, SKF, SB, HB, NS; Validation: GNK, TUPB, LSB, FG, FP, QRD, GZ, RM, HB; Visualization: GNK, TUPB, HB; Writing – original draft: GNK, TUPB, SB, HB, NS; Writing – review & editing: all authors.

Conflict of interest

NS has received speaker honoraria from Teva GmbH, Alexion Pharma Germany GmbH and Roche Pharma AG. RM is employed by the Buchinger Wilhelmi Development & Holding GmbH. The other authors declare no competing interests.

837 **Tables**

838 **Table 1.** Baseline characteristics of healthy participants depending on their randomization to
839 fasting and waiting control arm. Data are given as means (SD). p-values fasting vs. waiting by
840 t-test. BMI, body mass index; eGFR, estimated glomerular filtration rate; ALT, alanine
841 aminotransferase; TSH, thyroid-stimulating hormone; CRP, C-reactive protein; HbA1c,
842 glycated hemoglobin.

Variable	**All**	**Fasting**	**Waiting**	***P* value**
Number (n)	38	19	19	
Sex, female	19 / 38 (50%)	9 / 19 (47%)	10 / 19 (53%)	>0.9
Age (years)	38 (8)	39 (9)	36 (8)	0.4
BMI (kg/m^2)	25.1 (2.5)	25.0 (2.7)	25.2 (2.3)	0.7
eGFR (ml/min/1.73m^2)	102 (14)	98 (12)	106 (15)	0.1
ALT (U/l)	23.1 (8.1)	23.0 (8.2)	23.2 (8.2)	0.2
TSH (mU/l)	1.70 (0.84)	1.77 (0.91)	1.64 (0.77)	0.6
CRP (mg/dl)	0.98 (0.87)	0.78 (0.28)	1.17 (1.17)	0.2
Cholesterol (mg/dl)	182 (36)	189 (35)	175 (36)	0.2
HbA1c (mmol/mol)	33.2 (2.8)	34.2 (2.6)	32.3 (2.7)	0.03
Hemoglobin (g/dl)	14.0 (1.3)	13.8 (1.3)	14.2 (1.2)	0.41
White blood count (uL^{-1})	5.46 (1.02)	5.56 (0.96)	5.37 (1.09)	0.6
Thrombocytes (uL^{-1})	240 (42)	238 (63)	239 (54)	0.9

843

Table 2. Summary of predictive performance metrics for the predefined sparse 4-feature model, evaluated using 100 iterations of stratified 80/20 Monte Carlo resampling. Values are reported as mean ± SD across resamples. AUC, area under the receiver operating characteristic curve; F1, F1 score (harmonic mean of precision and recall); MCC, Matthews correlation coefficient; SD, standard deviation.

Metric	**Value (mean ± SD)**
AUC	0.84 ± 0.17
Accuracy	0.76 ± 0.15
Sensitivity	0.56 ± 0.34
Specificity	0.85 ± 0.17
Balanced Accuracy	0.71 ± 0.18
F1	0.68 ± 0.18
MCC	0.50 ± 0.35

850 **Table 3:** Comparison of predictive performance of clinical-only versus clinical+microbiome
851 models. Predictive performance of models trained on clinical features alone compared with
852 models including both clinical and microbiome features. Values represent mean ± SD across
853 100 repeated stratified 80/20 resamples. Inclusion of microbiome data improved
854 classification metrics across all performance measures, indicating additional predictive value
855 beyond clinical covariates. AUC, area under the receiver operating characteristic curve; SD,
856 standard deviation; F1, F1-score; MCC, Matthews correlation coefficient.

Metric	**Clinical-only model**	**Clinical + Microbiome model**
AUC	0.69 ± 0.21	0.86 ± 0.17
Accuracy	0.66 ± 0.18	0.74 ± 0.16
Sensitivity	0.52 ± 0.34	0.66 ± 0.35
Specificity	0.73 ± 0.22	0.78 ± 0.19
Balanced Accuracy	0.62 ± 0.19	0.72 ± 0.18
F1	0.60 ± 0.18	0.69 ± 0.16
MCC	0.28 ± 0.41	0.48 ± 0.37

857

858 **Figures**

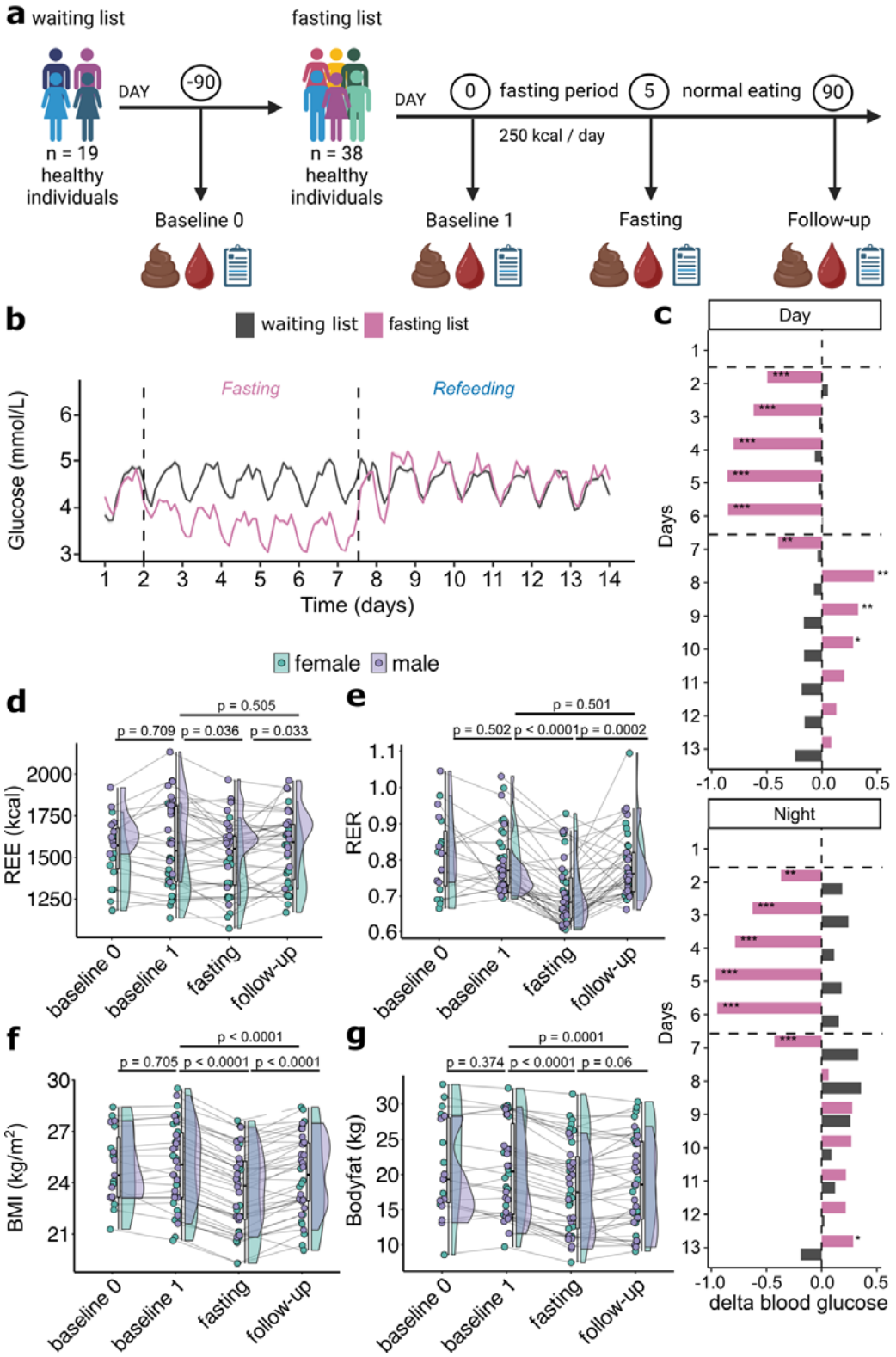

859

860 **Figure 1. Physiological effects of prolonged fasting in healthy individuals. a)** Schematic

861 overview of the randomized waitlist-controlled trial. A total of 38 healthy participants were

recruited. The first 19 participants immediately underwent prolonged fasting, while the remaining 19 served as a waitlist control group. After the initial intervention period, the waitlist group also underwent the same prolonged fasting protocol, resulting in a complete dataset of 38 participants undergoing prolonged fasting. The fasting intervention consisted of a 5-day period with 250 kcal/day, preceded and followed by baseline and follow-up visits at days 0, 5, and 90. Stool, blood, and clinical data were collected at each visit. The waitlist group was assessed at an additional baseline (day -90) to control for temporal fluctuations. **b)** Glucose time series measured by continuous intradermal monitoring starting one day prior to fasting (pink) or at baseline for the waiting list control (grey). **c)** Quantification of absolute changes in mmol/L of mean daytime (6am to 10pm) (top) and night (10pm to 6am) glucose levels (bottom), with changes compared to the individual baseline (day 1). Paired t-test with Benjamini-Hochberg false discovery rate correction (BH-FDR), *q<0.1, **q < 0.01, ***q < 0.001. **d)** Resting energy expenditure (REE), **e)** respiratory exchange ratio (RER), **f)** body mass index (BMI), and **g)** body fat percentage at the different study visits. Each point represents one participant, lines connect individuals, boxplot (middle) for all participants, violins (right side) and dots coloured by sex. P-values are from Wilcoxon signed-rank tests and were corrected using the Holm method.

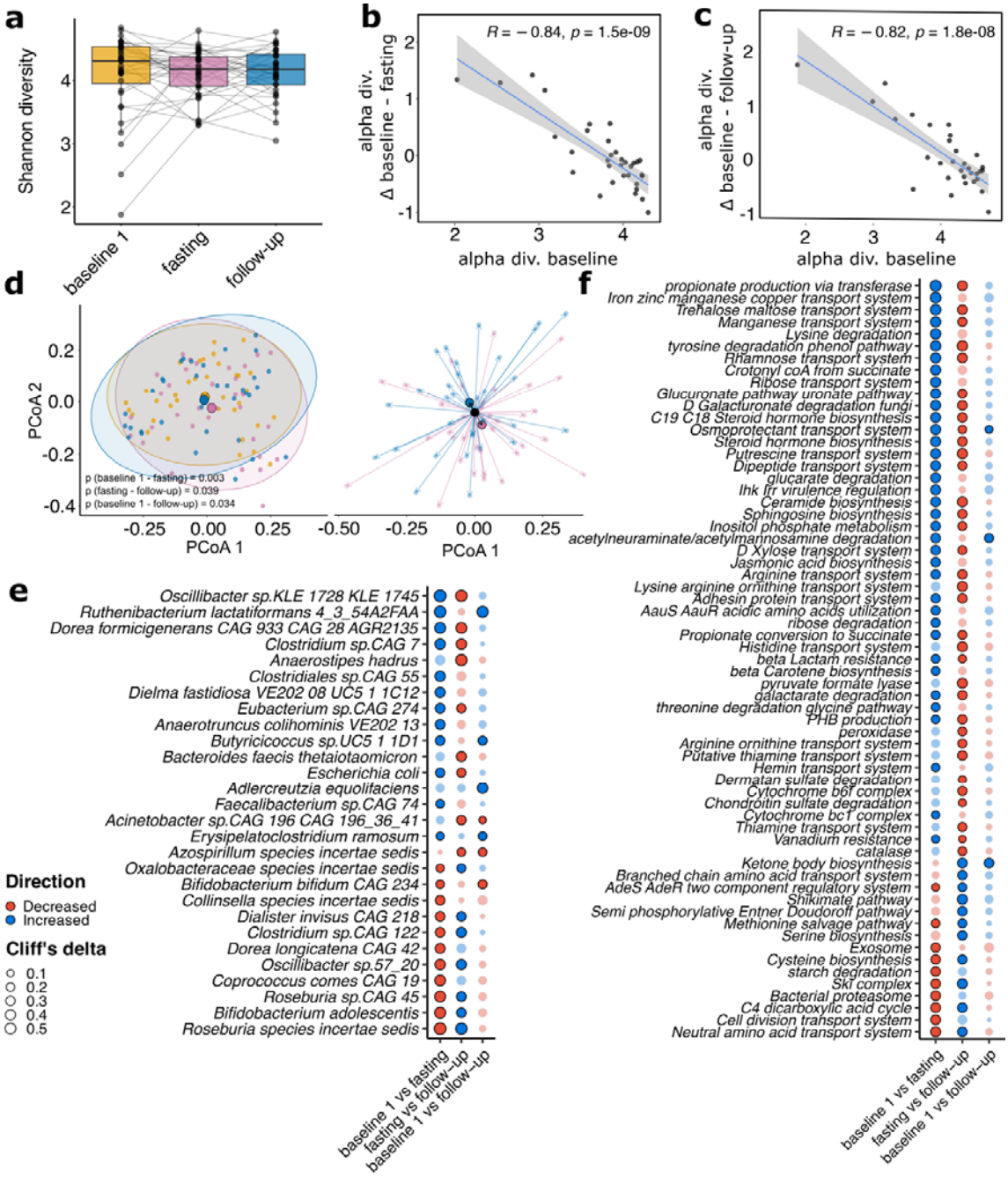

Figure 2. Prolonged fasting induces transient alterations in gut microbiome composition and function. a) Alpha diversity as measured by Shannon index for the study visits. Correlation of Shannon index at baseline with changes in Shannon index immediately **b)** post-fasting and **c)** at 12-week follow-up, indicating that baseline diversity predicts microbiome responsiveness. **d)** Principal coordinate analysis (PCoA) based on Bray–Curtis dissimilarity (naïve, left) and centered on baseline visit for fasting effect and on fasting visit

887 for post-fasting effect (right) show a transient shift in overall microbial composition after
888 fasting (pink), which partially reverts at follow-up (blue). Ellipses represent 95% confidence
889 intervals, p-values from PERMANOVA. Dot plots showing differential abundant **e)** species
890 (taxonomic level) and **f)** gut metabolic modules (functional level). Dots show fasting effects,
891 follow-up effects and study effects, transparency indicates non-significant findings (q>0.1),
892 dot size shows absolute Cliff's delta, color shows directionality. Significance by Wilcoxon
893 signed-rank test with Benjamini–Hochberg false discovery rate correction.
894

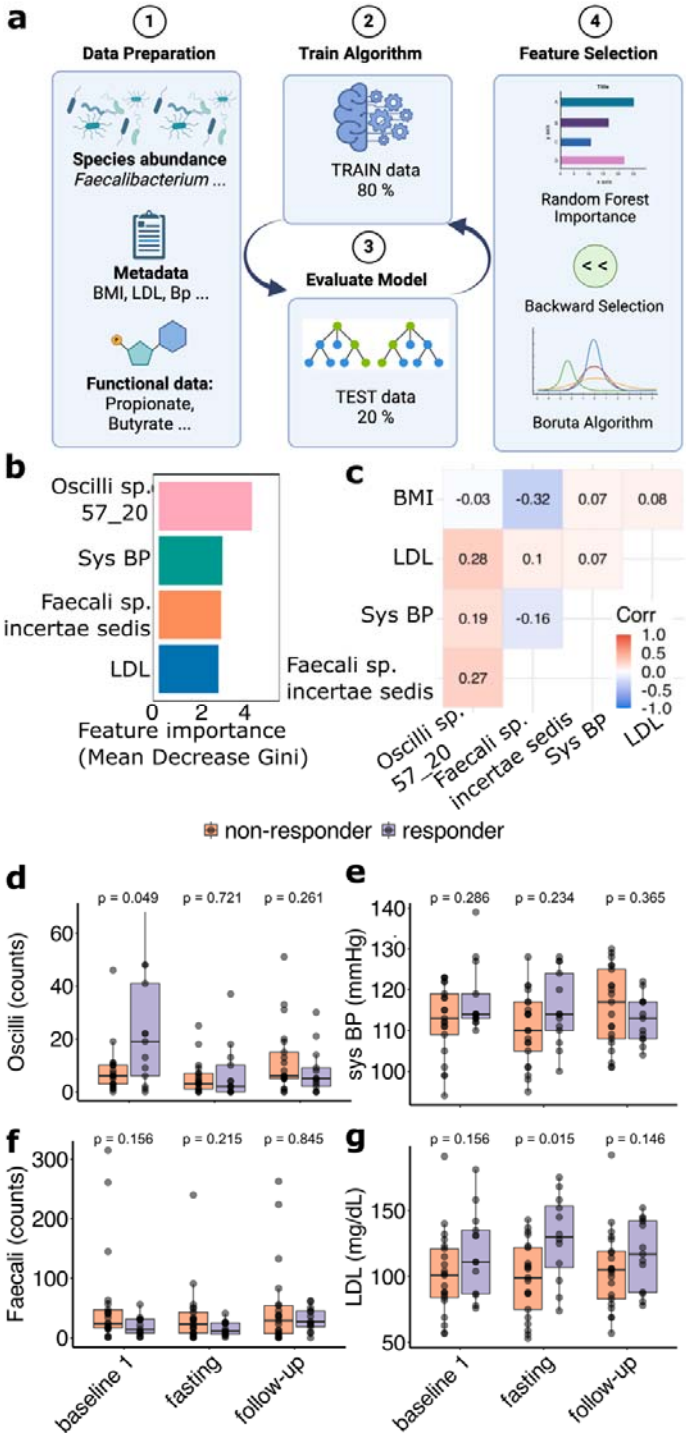

Figure 3. Machine learning model predicts sustained BMI response at follow-up to prolonged fasting using clinical and microbiome features. a) Schematic overview of the multi-*omics* feature selection and classification pipeline. Baseline species abundances, clinical metadata, and functional modules were used to train a random forest classifier.

900 Important features were selected through recursive feature elimination, Boruta algorithm,
901 and backward selection. **b)** Final model includes four top-ranked features: *Faecalibacterium*
902 sp. incertae sedis, *Oscillibacter* sp. 57_20, LDL cholesterol, and systolic blood pressure. **c)**
903 Correlation heatmap of the selected features showing independence from baseline BMI. R-
904 values from Spearman correlation. **d)** Boxplots of the four selected features at baseline,
905 comparing BMI responders and non-responders, dots show individual patients. P-values by
906 Mann-Whitney-U-test. Oscilli, *Oscillibacter* sp. 57_20; Faecali, *Faecalibacterium* sp. incertae
907 sedis; LDL, Low-density lipoprotein cholesterol; sys BP, systolic blood pressure.
908

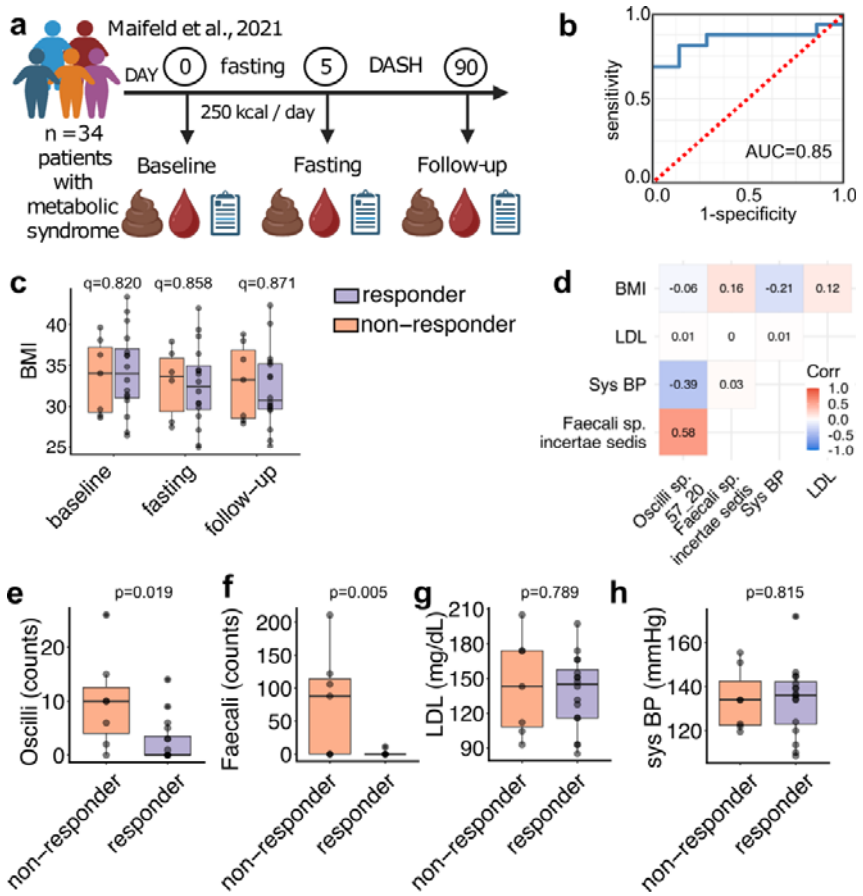

Figure 4. Application of BMI response prediction model in an external fasting cohort of patients with metabolic syndrome. a) Schematic of the Maifeld et al. (2021) study: 5-day fasting followed by a DASH diet in individuals with metabolic syndrome (n = 34), with BMI follow-up after 12 weeks. **b)** Receiver operating characteristic (ROC) curve of model performance in the external Maifeld cohort, showing good predictive accuracy (AUC = 0.85). **c)** BMI over the course of the study, split by participants classified as responders or non-responders. Each point represents a participant. P-values are from paired Wilcoxon signed-rank tests and were corrected for multiple comparisons using the Benjamini-Hochberg false discovery rate (FDR-BH) method. **d)** Correlation heatmap of model features with BMI. Features used for classification at baseline: **e)** *Oscillibacter* sp. 57_20, **f)** *Faecalibacterium* sp. incertae sedis, **g)** LDL, and **h)** systolic blood pressure. Oscilli, *Oscillibacter* sp. 57_20; Faecali,

921 *Faecalibacterium sp.* incertae sedis; LDL, Low-density lipoprotein cholesterol; sys BP, systolic

922 blood pressure.

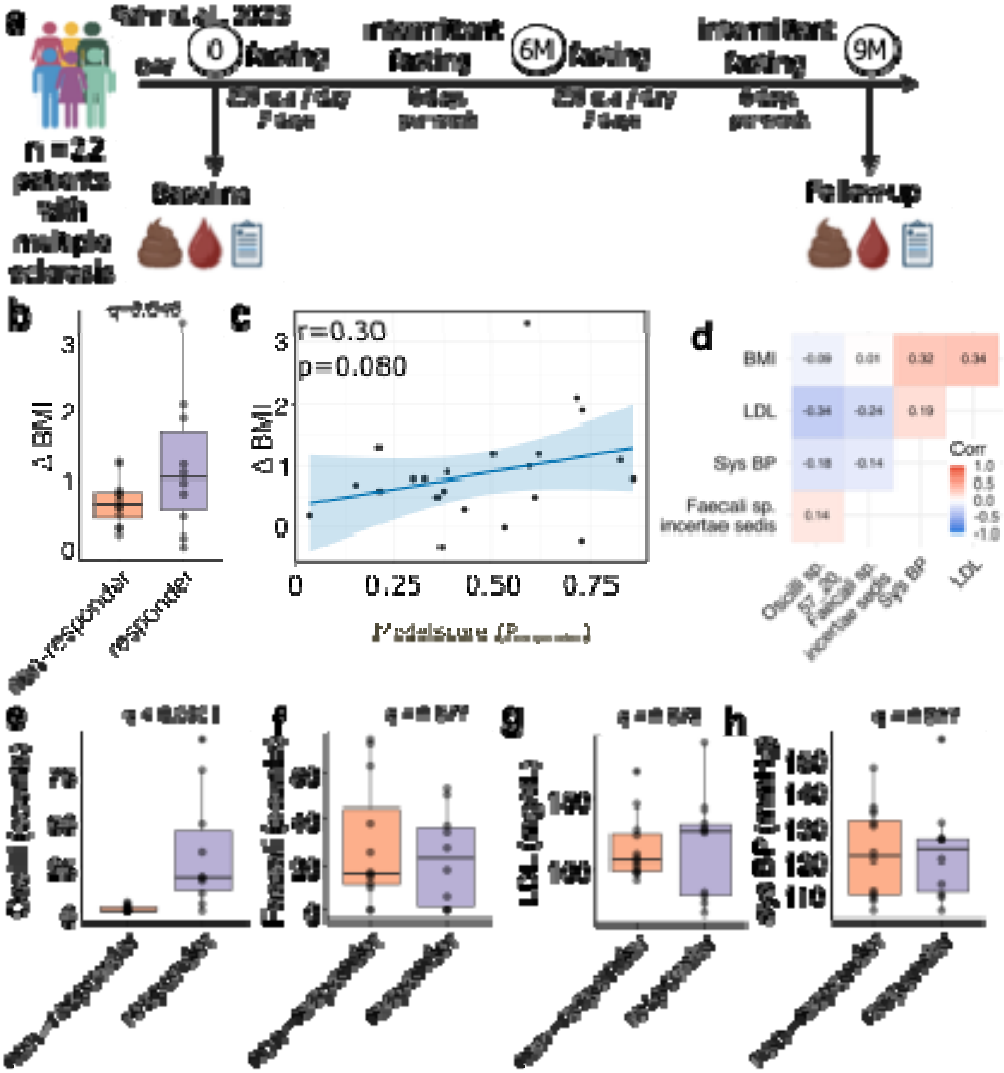

923

924 **Figure 5. Application of BMI response prediction model in an external fasting cohort of**

925 **patients with multiple sclerosis. a)** Schematic of the Bahr et al. (2025) study: two 7-day

926 periods of prolonged fasting and intermittent fasting in individuals with multiple sclerosis (n

927 = 22), over a 9-month period. **b)** BMI reduction at follow-up of patients classified as

928 responder or non-responder by the prediction model. p-value by one-tailed unpaired t-test.

929 **c)** Correlation analysis of changes in BMI with probability for responder status derived from

930 the model prediction. P-value by one-tailed Spearman correlation. **d)** Correlation heatmap of

931 model features with BMI. Features used for classification at baseline: **e)** *Oscillibacter* sp.
932 57_20, **f)** *Faecalibacterium* sp. incertae sedis, **g)** LDL, and **g)** systolic blood pressure. Oscilli,
933 *Oscillibacter* sp. 57_20; Faecali, *Faecalibacterium* sp. incertae sedis; LDL, Low-density
934 lipoprotein cholesterol; sys BP, systolic blood pressure.
935

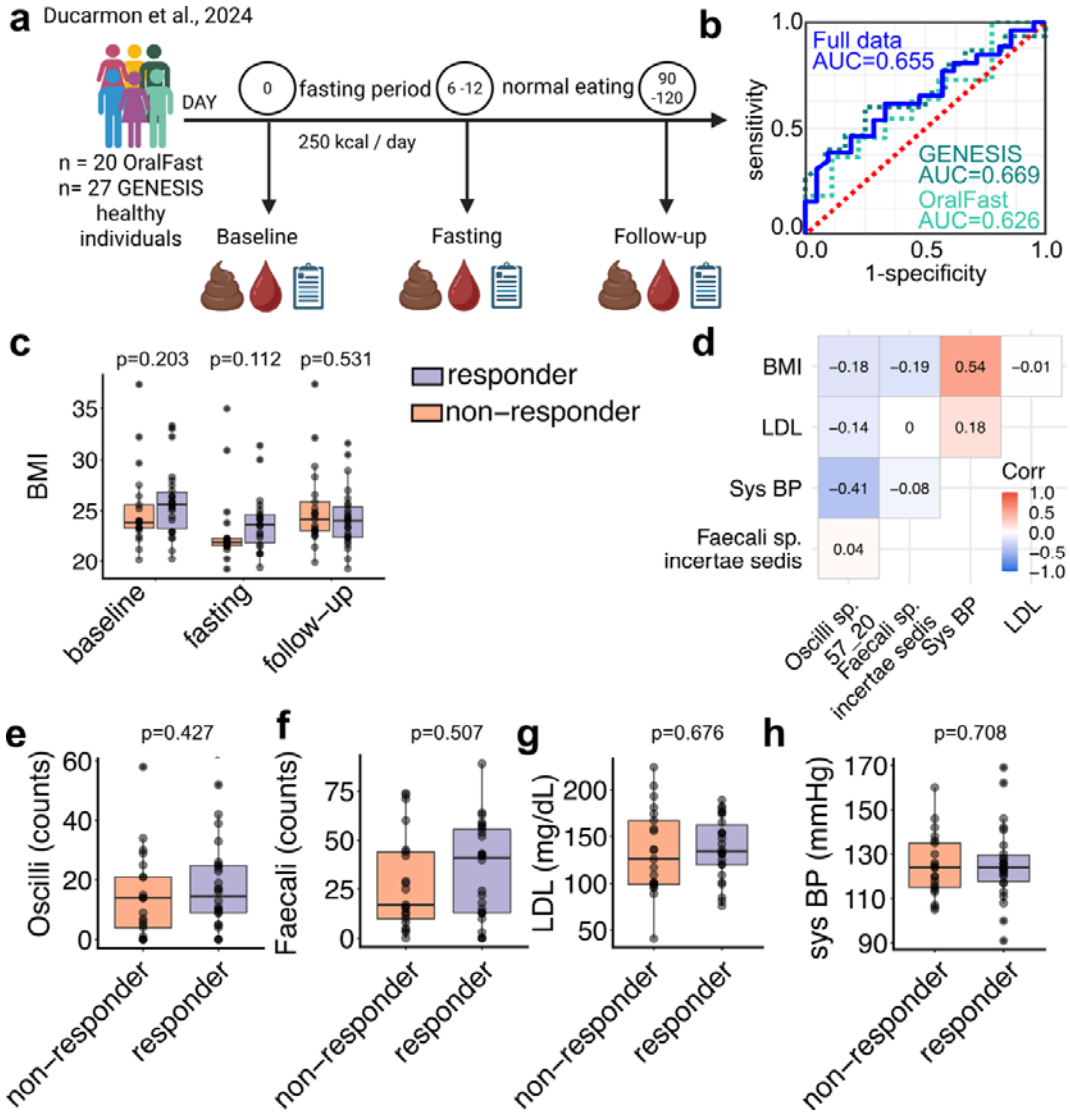

Figure 6. Application of BMI response prediction model in an external fasting cohort of healthy volunteers. a) Schematic of the Ducarmon et al. (2024) study: 6-12-days prolonged fasting with BMI follow-up after 3 months in the OralFast subcohort (n = 20) or 4 months in the GENESIS subcohort (n=27). **b)** Receiver operating characteristic (ROC) curve of model performance showing intermediate accuracy (AUC = 0.655). **c)** BMI over the course of the study, split by participants classified as responders or non-responders. Each point represents a participant. P-values are from paired Wilcoxon signed-rank tests and were corrected for multiple comparisons using the Benjamini-Hochberg false discovery rate (FDR-BH) method. **d)** Correlation heatmap of model features with BMI. Features used for classification at

946 baseline: **e)** *Oscillibacter* sp. 57_20, **f)** *Faecalibacterium* sp. incertae sedis, **g)** LDL, and **h)**

947 systolic blood pressure. Oscilli, *Oscillibacter* sp. 57_20; Faecali, *Faecalibacterium* sp. incertae

948 sedis; LDL, Low-density lipoprotein cholesterol; sys BP, systolic blood pressure.

949

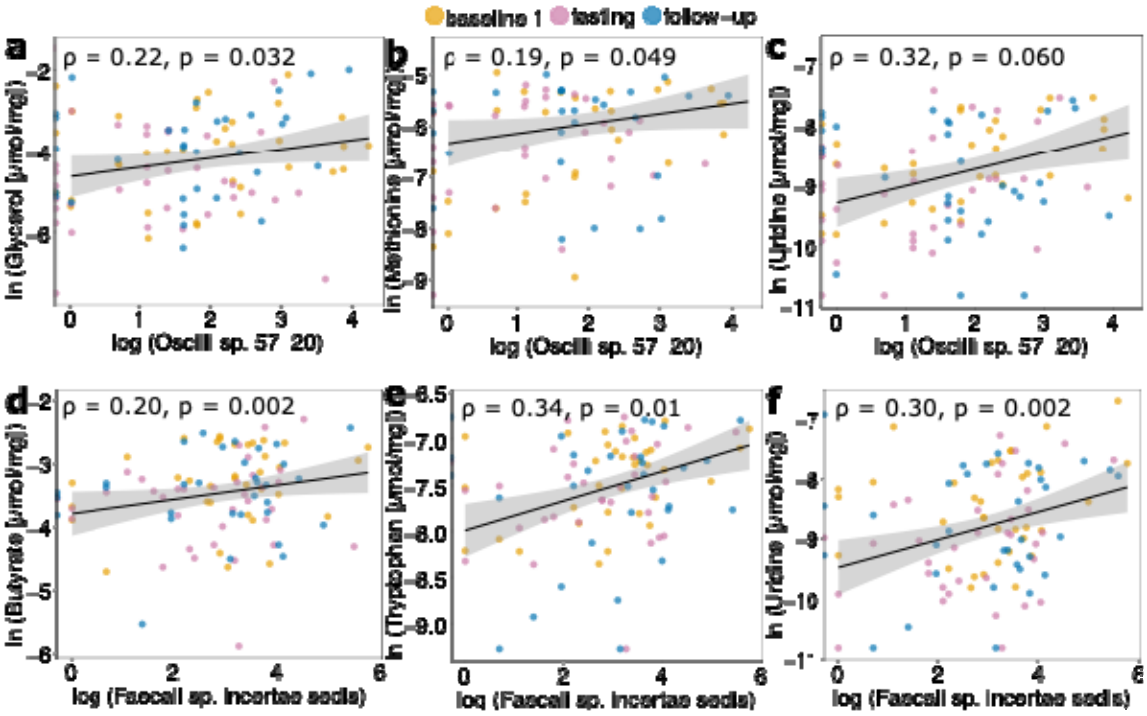

Figure 7. *Oscillibacter* sp. 57_20 and *Faecalibacterium* sp. incertae sedis abundance correlates with fecal metabolome. Correlation of *Oscillibacter* (Oscilli) sp. 57_20 abundance with fecal **a)** glycerol, **b)** methionine, and **c)** uridine levels. Correlation of *Faecalibacterium* (Faecali) sp. incertae sedis abundance with fecal **d)** butyrate, **e)** tryptophan, and **f)** uridine levels. R-values from Spearman's correlation. P-values from permutation-based independence test screening for associations of species with metabolites while blocking effects of study visits. Abbreviations: Oscilli: *Oscillibacter* sp. 57_20; Faecali: *Faecalibacterium* sp. incertae sedis.

961 **References**

962 1 Di Francesco, A., Di Germanio, C., Bernier, M. & de Cabo, R. A time to fast. *Science*
963 **362**, 770-775 (2018). https://doi.org:10.1126/science.aau2095

964 2 Brandhorst, S. *et al.* Fasting-mimicking diet causes hepatic and blood markers changes
965 indicating reduced biological age and disease risk. *Nat Commun* **15**, 1309 (2024).
966 https://doi.org:10.1038/s41467-024-45260-9

967 3 Gewecke, K. *et al.* Long-term fasting induces a remodelling of fatty acid composition
968 in erythrocyte membranes. *Eur J Clin Invest*, e14382 (2025).
969 https://doi.org:10.1111/eci.14382

970 4 Koppold, D. A. *et al.* International consensus on fasting terminology. *Cell Metab* **36**,
971 1779-1794 e1774 (2024). https://doi.org:10.1016/j.cmet.2024.06.013

972 5 Maifeld, A. *et al.* Fasting alters the gut microbiome reducing blood pressure and body
973 weight in metabolic syndrome patients. *Nat Commun* **12**, 1970 (2021).
974 https://doi.org:10.1038/s41467-021-22097-0

975 6 Cignarella, F. *et al.* Intermittent Fasting Confers Protection in CNS Autoimmunity by
976 Altering the Gut Microbiota. *Cell Metab* **27**, 1222-1235 e1226 (2018).
977 https://doi.org:10.1016/j.cmet.2018.05.006

978 7 Choi, I. Y. *et al.* A Diet Mimicking Fasting Promotes Regeneration and Reduces
979 Autoimmunity and Multiple Sclerosis Symptoms. *Cell Rep* **15**, 2136-2146 (2016).
980 https://doi.org:10.1016/j.celrep.2016.05.009

981 8 de Groot, S. *et al.* Fasting mimicking diet as an adjunct to neoadjuvant chemotherapy
982 for breast cancer in the multicentre randomized phase 2 DIRECT trial. *Nat Commun*
983 **11**, 3083 (2020). https://doi.org:10.1038/s41467-020-16138-3

984 9 National Academies of Sciences, E. & Medicine. *Dietary Reference Intakes for Energy*.
985 (The National Academies Press, 2023).
986 10 Weyer, C., Snitker, S., Rising, R., Bogardus, C. & Ravussin, E. Determinants of energy
987 expenditure and fuel utilization in man: effects of body composition, age, sex,
988 ethnicity and glucose tolerance in 916 subjects. *Int J Obes Relat Metab Disord* **23**,
989 715-722 (1999). https://doi.org:10.1038/sj.ijo.0800910
990 11 Delsoglio, M., Achamrah, N., Berger, M. M. & Pichard, C. Indirect Calorimetry in
991 Clinical Practice. *J Clin Med* **8** (2019). https://doi.org:10.3390/jcm8091387
992 12 Levine, J. A. Measurement of energy expenditure. *Public Health Nutr* **8**, 1123-1132
993 (2005). https://doi.org:10.1079/phn2005800
994 13 Ratiner, K., Ciocan, D., Abdeen, S. K. & Elinav, E. Utilization of the microbiome in
995 personalized medicine. *Nat Rev Microbiol* **22**, 291-308 (2024).
996 https://doi.org:10.1038/s41579-023-00998-9
997 14 von Schwartzenberg, R. J. *et al.* Caloric restriction disrupts the microbiota and
998 colonization resistance. *Nature* **595**, 272-277 (2021). https://doi.org:10.1038/s41586-
999 021-03663-4
1000 15 Murthy, V. L. *et al.* Metabolic liability for weight gain in early adulthood. *Cell Rep Med*
1001 **5**, 101548 (2024). https://doi.org:10.1016/j.xcrm.2024.101548
1002 16 Jiang, Z. *et al.* Human gut microbial aromatic amino acid and related metabolites
1003 prevent obesity through intestinal immune control. *Nat Metab* **7**, 808-822 (2025).
1004 https://doi.org:10.1038/s42255-025-01246-5
1005 17 Hill, D. A. *et al.* Metagenomic analyses reveal antibiotic-induced temporal and spatial
1006 changes in intestinal microbiota with associated alterations in immune cell

1007 homeostasis. *Mucosal Immunol* **3**, 148-158 (2010).
1008 https://doi.org:10.1038/mi.2009.132
1009 18 Rakoff-Nahoum, S., Paglino, J., Eslami-Varzaneh, F., Edberg, S. & Medzhitov, R.
1010 Recognition of commensal microflora by toll-like receptors is required for intestinal
1011 homeostasis. *Cell* **118**, 229-241 (2004). https://doi.org:10.1016/j.cell.2004.07.002
1012 19 Zheng, J. *et al.* Noninvasive, microbiome-based diagnosis of inflammatory bowel
1013 disease. *Nat Med* **30**, 3555-3567 (2024). https://doi.org:10.1038/s41591-024-03280-4
1014 20 Darzi, Y., Falony, G., Vieira-Silva, S. & Raes, J. Towards biome-specific analysis of meta-
1015 omics data. *ISME J* **10**, 1025-1028 (2016). https://doi.org:10.1038/ismej.2015.188
1016 21 Ozarda, Y. *et al.* Protocol and standard operating procedures for common use in a
1017 worldwide multicenter study on reference values. *Clin Chem Lab Med* **51**, 1027-1040
1018 (2013). https://doi.org:10.1515/cclm-2013-0249
1019 22 Bahr, L. S. *et al.* Fasting, ketogenic, and anti-inflammatory diets in multiple sclerosis: a
1020 randomized controlled trial with 18-month follow-up. *BMC Nutr* **11**, 167 (2025).
1021 https://doi.org:10.1186/s40795-025-01156-5
1022 23 Ducarmon, Q. *et al.* Long-term fasting remodels gut microbial metabolism and host
1023 metabolism. *bioRxiv*, 2024.2004.2019.590209 (2024).
1024 https://doi.org:10.1101/2024.04.19.590209
1025 24 Hothorn, T., Hornik, K., van de Wiel, M. A. & Zeileis, A. Implementing a Class of
1026 Permutation Tests: The coin Package. *Journal of Statistical Software* **28**, 1 - 23 (2008).
1027 https://doi.org:10.18637/jss.v028.i08
1028 25 Berry, S. E. *et al.* Human postprandial responses to food and potential for precision
1029 nutrition. *Nat Med* **26**, 964-973 (2020). https://doi.org:10.1038/s41591-020-0934-0

1030 26 Zeevi, D. *et al.* Personalized Nutrition by Prediction of Glycemic Responses. *Cell* **163**,
1031 1079-1094 (2015). https://doi.org:10.1016/j.cell.2015.11.001
1032 27 Horton, T. J. & Hill, J. O. Prolonged fasting significantly changes nutrient oxidation and
1033 glucose tolerance after a normal mixed meal. *J Appl Physiol (1985)* **90**, 155-163
1034 (2001). https://doi.org:10.1152/jappl.2001.90.1.155
1035 28 Solianik, R., Zidoniene, K., Eimantas, N. & Brazaitis, M. Prolonged fasting outperforms
1036 short-term fasting in terms of glucose tolerance and insulin release: a randomised
1037 controlled trial. *Br J Nutr* **130**, 1500-1509 (2023).
1038 https://doi.org:10.1017/S0007114523000557
1039 29 Laurens, C. *et al.* Is muscle and protein loss relevant in long-term fasting in healthy
1040 men? A prospective trial on physiological adaptations. *J Cachexia Sarcopenia Muscle*
1041 **12**, 1690-1703 (2021). https://doi.org:10.1002/jcsm.12766
1042 30 Dai, Z. *et al.* Effects of 10-Day Complete Fasting on Physiological Homeostasis,
1043 Nutrition and Health Markers in Male Adults. *Nutrients* **14** (2022).
1044 https://doi.org:10.3390/nu14183860
1045 31 Triffoni-Melo, A. T., Suen, V. M. M., Resende, C. M. M., Braga, C. B. M. & Diez-Garcia,
1046 R. W. Resting energy expenditure adaptation after short-term caloric restriction in
1047 morbidly obese women. *Rev Nutr* **28**, 505-511 (2015). https://doi.org:10.1590/1415-
1048 52732015000500005
1049 32 Schlogl, M. *et al.* Energy Expenditure Responses to Fasting and Overfeeding Identify
1050 Phenotypes Associated With Weight Change. *Diabetes* **64**, 3680-3689 (2015).
1051 https://doi.org:10.2337/db15-0382
1052 33 Mohr, A. E. *et al.* Gut microbiome remodeling and metabolomic profile improves in
1053 response to protein pacing with intermittent fasting versus continuous caloric

1054 restriction. *Nat Commun* **15**, 4155 (2024). https://doi.org:10.1038/s41467-024-
1055 48355-5
1056 34 Hodge, J. M., Shah, R., McCullough, M. L., Gapstur, S. M. & Patel, A. V. Validation of
1057 self-reported height and weight in a large, nationwide cohort of U.S. adults. *PLoS One*
1058 **15**, e0231229 (2020). https://doi.org:10.1371/journal.pone.0231229
1059 35 Longo, V. D. & Mattson, M. P. Fasting: molecular mechanisms and clinical applications.
1060 *Cell Metab* **19**, 181-192 (2014). https://doi.org:10.1016/j.cmet.2013.12.008
1061 36 Van Calster, B. *et al*. Calibration: the Achilles heel of predictive analytics. *BMC Med*
1062 **17**, 230 (2019). https://doi.org:10.1186/s12916-019-1466-7
1063 37 Schurz, H. *et al.* Simulating mismatch between calibration and target population in AI
1064 for mammography the retrospective VAIB study. *NPJ Digit Med* **8**, 259 (2025).
1065 https://doi.org:10.1038/s41746-025-01623-0
1066 38 Pudjihartono, N., Fadason, T., Kempa-Liehr, A. W. & O'Sullivan, J. M. A Review of
1067 Feature Selection Methods for Machine Learning-Based Disease Risk Prediction. *Front*
1068 *Bioinform* **2**, 927312 (2022). https://doi.org:10.3389/fbinf.2022.927312
1069 39 Huynh-Thu, V. A., Saeys, Y., Wehenkel, L. & Geurts, P. Statistical interpretation of
1070 machine learning-based feature importance scores for biomarker discovery.
1071 *Bioinformatics* **28**, 1766-1774 (2012). https://doi.org:10.1093/bioinformatics/bts238
1072 40 Karwowska, Z., Aasmets, O., Estonian Biobank research, t., Kosciolek, T. & Org, E.
1073 Effects of data transformation and model selection on feature importance in
1074 microbiome classification data. *Microbiome* **13**, 2 (2025).
1075 https://doi.org:10.1186/s40168-024-01996-6

1076 41 Fromentin, S. *et al.* Microbiome and metabolome features of the cardiometabolic
1077 disease spectrum. *Nat Med* **28**, 303-314 (2022). https://doi.org:10.1038/s41591-022-
1078 01688-4
1079 42 Wang, Y. C. *et al.* Indole-3-Propionic Acid Protects Against Heart Failure With
1080 Preserved Ejection Fraction. *Circ Res* **134**, 371-389 (2024).
1081 https://doi.org:10.1161/CIRCRESAHA.123.322381
1082 43 Barcenilla, A. *et al.* Phylogenetic relationships of butyrate-producing bacteria from
1083 the human gut. *Appl Environ Microbiol* **66**, 1654-1661 (2000).
1084 https://doi.org:10.1128/AEM.66.4.1654-1661.2000
1085 44 Essex, M. *et al.* Gut microbiota dysbiosis is associated with altered tryptophan
1086 metabolism and dysregulated inflammatory response in COVID-19. *NPJ Biofilms*
1087 *Microbiomes* **10**, 66 (2024). https://doi.org:10.1038/s41522-024-00538-0
1088 45 Roager, H. M. & Licht, T. R. Microbial tryptophan catabolites in health and disease.
1089 *Nat Commun* **9**, 3294 (2018). https://doi.org:10.1038/s41467-018-05470-4
1090 46 Hanssen, R. *et al.* Circulating uridine dynamically and adaptively regulates food intake
1091 in humans. *Cell Rep Med* **4**, 100897 (2023).
1092 https://doi.org:10.1016/j.xcrm.2022.100897
1093 47 Deng, Y. *et al.* An adipo-biliary-uridine axis that regulates energy homeostasis. *Science*
1094 **355** (2017). https://doi.org:10.1126/science.aaf5375
1095 48 Steculorum, S. M. *et al.* Hypothalamic UDP Increases in Obesity and Promotes
1096 Feeding via P2Y6-Dependent Activation of AgRP Neurons. *Cell* **162**, 1404-1417 (2015).
1097 https://doi.org:10.1016/j.cell.2015.08.032
1098 49 Deng, Y. *et al.* Adipocyte Xbp1s overexpression drives uridine production and reduces
1099 obesity. *Mol Metab* **11**, 1-17 (2018). https://doi.org:10.1016/j.molmet.2018.02.013

1100 50 Han, H. *et al.* From gut microbiota to host appetite: gut microbiota-derived
1101 metabolites as key regulators. *Microbiome* **9**, 162 (2021).
1102 https://doi.org:10.1186/s40168-021-01093-y
1103 51 Ali, I. *et al.* Ramadan Fasting Leads to Shifts in Human Gut Microbiota Structured by
1104 Dietary Composition. *Front Microbiol* **12**, 642999 (2021).
1105 https://doi.org:10.3389/fmicb.2021.642999
1106 52 Lopez-Siles, M., Duncan, S. H., Garcia-Gil, L. J. & Martinez-Medina, M.
1107 Faecalibacterium prausnitzii: from microbiology to diagnostics and prognostics. *ISME*
1108 *J* **11**, 841-852 (2017). https://doi.org:10.1038/ismej.2016.176
1109 53 Remely, M. *et al.* Increased gut microbiota diversity and abundance of
1110 Faecalibacterium prausnitzii and Akkermansia after fasting: a pilot study. *Wien Klin*
1111 *Wochenschr* **127**, 394-398 (2015). https://doi.org:10.1007/s00508-015-0755-1
1112 54 Guo, Y. *et al.* Intermittent Fasting Improves Cardiometabolic Risk Factors and Alters
1113 Gut Microbiota in Metabolic Syndrome Patients. *J Clin Endocrinol Metab* **106**, 64-79
1114 (2021). https://doi.org:10.1210/clinem/dgaa644
1115 55 Mesnage, R., Grundler, F., Schwiertz, A., Le Maho, Y. & Wilhelmi de Toledo, F. Changes
1116 in human gut microbiota composition are linked to the energy metabolic switch
1117 during 10 d of Buchinger fasting. *J Nutr Sci* **8**, e36 (2019).
1118 https://doi.org:10.1017/jns.2019.33
1119 56 Ozkul, C., Yalinay, M. & Karakan, T. Structural changes in gut microbiome after
1120 Ramadan fasting: a pilot study. *Benef Microbes* **11**, 227-233 (2020).
1121 https://doi.org:10.3920/BM2019.0039

1122 57 Sinha, A. K. *et al.* Dietary fibre directs microbial tryptophan metabolism via metabolic
1123 interactions in the gut microbiota. *Nat Microbiol* **9**, 1964-1978 (2024).
1124 https://doi.org:10.1038/s41564-024-01737-3
1125 58 Fassarella, M. *et al.* Gut microbiome stability and resilience: elucidating the response
1126 to perturbations in order to modulate gut health. *Gut* **70**, 595-605 (2021).
1127 https://doi.org:10.1136/gutjnl-2020-321747
1128 59 Khan, M. N. *et al.* Intermittent fasting positively modulates human gut microbial
1129 diversity and ameliorates blood lipid profile. *Front Microbiol* **13**, 922727 (2022).
1130 https://doi.org:10.3389/fmicb.2022.922727
1131 60 Rajput, D., Wang, W. J. & Chen, C. C. Evaluation of a decided sample size in machine
1132 learning applications. *BMC Bioinformatics* **24**, 48 (2023).
1133 https://doi.org:10.1186/s12859-023-05156-9
1134 61 Birkenbihl, C. *et al.* Differences in cohort study data affect external validation of
1135 artificial intelligence models for predictive diagnostics of dementia - lessons for
1136 translation into clinical practice. *EPMA J* **11**, 367-376 (2020).
1137 https://doi.org:10.1007/s13167-020-00216-z
1138 62 Harris, P. A. *et al.* The REDCap consortium: Building an international community of
1139 software platform partners. *J Biomed Inform* **95**, 103208 (2019).
1140 https://doi.org:10.1016/j.jbi.2019.103208
1141 63 Harris, P. A. *et al.* Research electronic data capture (REDCap)--a metadata-driven
1142 methodology and workflow process for providing translational research informatics
1143 support. *J Biomed Inform* **42**, 377-381 (2009).
1144 https://doi.org:10.1016/j.jbi.2008.08.010

1145 64 Hopewell, S. *et al.* CONSORT 2025 statement: updated guideline for reporting
1146 randomised trials. *BMJ* **389**, e081123 (2025). https://doi.org:10.1136/bmj-2024-
1147 081123
1148 65 Mahler, A. *et al.* Increased Salt Intake Decreases Diet-Induced Thermogenesis in
1149 Healthy Volunteers: A Randomized Placebo-Controlled Study. *Nutrients* **14** (2022).
1150 https://doi.org:10.3390/nu14020253
1151 66 Bartolomaeus, T. U. P. *et al.* Quantifying technical confounders in microbiome studies.
1152 *Cardiovasc Res* **117**, 863-875 (2021). https://doi.org:10.1093/cvr/cvaa128
1153